



**University of Dundee**

## **Loop G in the GABAA receptor 1 subunit influences gating efficacy**

Baptista-Hon, Daniel T.; Gulbinaite, Simona; Hales, Tim G.

*Published in:*  
Journal of Physiology

*DOI:*  
[10.1113/JP273752](https://doi.org/10.1113/JP273752)

*Publication date:*  
2017

*Document Version*  
Peer reviewed version

[Link to publication in Discovery Research Portal](#)

### *Citation for published version (APA):*

Baptista-Hon, D. T., Gulbinaite, S., & Hales, T. G. (2017). Loop G in the GABAA receptor 1 subunit influences gating efficacy. *Journal of Physiology*, 595(5), 1725-1741. <https://doi.org/10.1113/JP273752>

### **General rights**

Copyright and moral rights for the publications made accessible in Discovery Research Portal are retained by the authors and/or other copyright owners and it is a condition of accessing publications that users recognise and abide by the legal requirements associated with these rights.

- Users may download and print one copy of any publication from Discovery Research Portal for the purpose of private study or research.
- You may not further distribute the material or use it for any profit-making activity or commercial gain.
- You may freely distribute the URL identifying the publication in the public portal.

### **Take down policy**

If you believe that this document breaches copyright please contact us providing details, and we will remove access to the work immediately and investigate your claim.

## Loop G in the GABA<sub>A</sub> receptor $\alpha$ 1 subunit influences gating efficacy

Abbreviated title: GABA<sub>A</sub>R loop G in gating

Daniel T. Baptista-Hon, Simona Gulbinaite & Tim G. Hales\*

The Institute of Academic Anaesthesia, Division of Neuroscience, School of Medicine, Ninewells Hospital, University of Dundee, Dundee, DD1 9SY, UK,

\*Corresponding author. E-mail: [t.g.hales@dundee.ac.uk](mailto:t.g.hales@dundee.ac.uk)

Key words: Cys-loop receptors, mutagenesis, spontaneous gating, pentameric ligand-gated ion channels

### Key points summary

- The functional importance of residues in loop G of the GABA<sub>A</sub> receptor has not been investigated. D43 and T47 in the  $\alpha$ 1 subunit are of particular significance as their structural modification inhibits activation by GABA.
- While the T47C substitution had no significant effect, non-conservative substitution of either residue (D43C and T47R) reduced the apparent potency of GABA.
- Propofol potentiated maximal GABA-evoked currents mediated by  $\alpha$ 1(D43C) $\beta$ 2 $\gamma$ 2 and  $\alpha$ 1(T47R) $\beta$ 2 $\gamma$ 2 receptors. Non-stationary variance analysis revealed a reduction in maximal GABA-evoked  $P_{open}$ , suggesting impaired agonist efficacy.
- Further analysis of  $\alpha$ 1(T47R) $\beta$ 2 $\gamma$ 2 receptors revealed that the efficacy of the partial agonist THIP relative to GABA was impaired.
- GABA-, THIP- and propofol-evoked currents mediated by  $\alpha$ 1(T47R) $\beta$ 2 $\gamma$ 2 receptors deactivated faster than those mediated by  $\alpha$ 1 $\beta$ 2 $\gamma$ 2 receptors indicating that the mutation impairs agonist-evoked gating.

This is an Accepted Article that has been peer-reviewed and approved for publication in the The Journal of Physiology, but has yet to undergo copy-editing and proof correction. Please cite this article as an 'Accepted Article'; [doi: 10.1113/JP273752](https://doi.org/10.1113/JP273752).

This article is protected by copyright. All rights reserved.

- Spontaneous gating caused by the  $\beta 2(L285R)$  mutation was also reduced in  $\alpha 1(T47R)\beta 2(L285R)\gamma 2$  compared to  $\alpha 1\beta 2(L285R)\gamma 2$  receptors confirming that  $\alpha 1(T47R)$  impairs gating independently of agonist activation.

**Abstract**

The modification of Cys residues (substituted for D43 and T47) by 2-aminoethyl methanethiosulfonate in the GABA<sub>A</sub>  $\alpha$ 1 subunit loop G impairs activation of  $\alpha$ 1 $\beta$ 2 $\gamma$ 2 receptors by GABA and propofol (Baptista-Hon *et al.*, 2016). While the T47C substitution had no significant effect, non-conservative substitution of either residue (D43C and T47R) reduced the apparent potency of GABA. Propofol (1  $\mu$ M), which potentiates sub-maximal, but not maximal GABA-evoked currents mediated by  $\alpha$ 1 $\beta$ 2 $\gamma$ 2 receptors, also potentiated maximal currents mediated by  $\alpha$ 1(D43C) $\beta$ 2 $\gamma$ 2 and  $\alpha$ 1(T47R) $\beta$ 2 $\gamma$ 2 receptors. Furthermore, the peak open probabilities of  $\alpha$ 1(D43C) $\beta$ 2 $\gamma$ 2 and  $\alpha$ 1(T47R) $\beta$ 2 $\gamma$ 2 receptors were reduced. The kinetics of macroscopic currents mediated by  $\alpha$ 1(D43C) $\beta$ 2 $\gamma$ 2 and  $\alpha$ 1(T47R) $\beta$ 2 $\gamma$ 2 receptors were characterised by slower desensitisation and faster deactivation. Similar changes in macroscopic current kinetics, together with a slower activation rate, were observed with the loop D  $\alpha$ 1(F64C) substitution, known to impair both efficacy and agonist binding, and when the partial agonist THIP was used to activate WT or  $\alpha$ 1(T47R) $\beta$ 2 $\gamma$ 2 receptors. Propofol-evoked currents mediated by  $\alpha$ 1(T47R) $\beta$ 2 $\gamma$ 2 and  $\alpha$ 1(F64C) $\beta$ 2 $\gamma$ 2 receptors also exhibited faster deactivation than their WT counterparts revealing that these substitutions impair gating through a mechanism independent of orthosteric binding. Spontaneous gating caused by the introduction of the  $\beta$ 2(L285R) mutation was also reduced in  $\alpha$ 1(T47R) $\beta$ 2(L285R) $\gamma$ 2 compared to  $\alpha$ 1 $\beta$ 2(L285R) $\gamma$ 2 receptors confirming that  $\alpha$ 1(T47R) impairs gating independently of activation by any agonist. These findings implicate movement of the GABA<sub>A</sub> receptor  $\alpha$ 1 subunit's  $\beta$ 1 strand during agonist dependent and spontaneous gating. Immobilisation of the  $\beta$ 1 strand may provide a mechanism for the inhibition of gating by inverse agonists such as bicuculline.

**Abbreviations list**

DMEM, Dulbecco modified Eagle's medium; GABA,  $\gamma$ -aminobutyric acid; GluCl, glutamate-activated Cl<sup>-</sup> channel; HEK-293, human embryonic kidney 293 cell; MD, molecular dynamic; MTSEA, 2-aminoethyl methanethiosulfonate; pLGIC, pentameric ligand-gated ion channel; THIP, 4,5,6,7-tetrahydroisoxazolo[5,4-c]pyridine-3-ol; TM, transmembrane;  $\tau_w$ , weighted tau.

## Introduction

$\gamma$ -Aminobutyric acid type A (GABA<sub>A</sub>) receptors are Cys-loop receptors of the pentameric ligand-gated ion channel (pLGIC) family. They mediate fast inhibitory neurotransmission. Nineteen different genes encode GABA<sub>A</sub> receptor subunits, providing considerable heterogeneity in GABA<sub>A</sub> receptor composition. The most abundant GABA<sub>A</sub> receptors in the brain are comprised of  $\alpha$ 1,  $\beta$ 2 and  $\gamma$ 2 subunits (Whiting et al., 1995).

In common with other pLGICs, GABA<sub>A</sub> receptors have an N-terminal extracellular domain, which contains the orthosteric agonist binding site and four transmembrane (TM) domains (TM1-4) containing additional binding sites for positive modulators and allosteric agonists, such as the general anaesthetic propofol. The Cl<sup>-</sup>-selective channel pore, containing the gate, is encompassed by five TM2 domains arranged pseudo-symmetrically (Miller & Aricescu, 2014). The intracellular domains of pLGICs are generally large, being mostly composed of the TM3-4 loop (Baptista-Hon et al., 2013). TM domains are most highly conserved across pLGICs, while the intracellular loops are highly heterogeneous.

The orthosteric binding site of the GABA<sub>A</sub> receptor is located in the N-terminal domain between adjacent  $\alpha$ - and  $\beta$ - subunits (Smith & Olsen, 1995; Cromer *et al.*, 2002). In this region, seven non-contiguous loops (A-G) line the orthosteric site, where they participate in agonist binding (Boileau *et al.*, 1999; Holden & Czajkowski, 2002; Wagner *et al.*, 2004; Goldschen-Ohm *et al.*, 2011; Tran *et al.*, 2011) and/or gating (Boileau *et al.*, 2002; Newell & Czajkowski, 2003; Venkatachalan & Czajkowski, 2008; Szczot *et al.*, 2014; Baptista-Hon *et al.*, 2016). These loops are contained within an anti-parallel  $\beta$  sandwich structure. In the canonical  $\alpha$ 1 $\beta$ 2 $\gamma$ 2 GABA<sub>A</sub> receptor, loops A, B and C are contributed by the primary interface, from the  $\beta$ 2 subunit, while loops D, E, F and loop G are contributed by the complementary interface, from the  $\alpha$ 1 subunit.

Arg37 in loop G was recently identified for its role in glutamate binding to the *Caenorhabditis elegans* glutamate-activated Cl<sup>-</sup> (GluCl) pLGIC (Hibbs & Gouaux, 2011). However, residues in this region are not implicated in binding agonists to other pLGICs, such as the GABA<sub>A</sub>  $\beta$ 3 homopentamer (Miller & Aricescu, 2014), the glycine receptor (Du *et al.*, 2015) or the  $\alpha$ 4 $\beta$ 2 nicotinic acetylcholine receptor (Morales-Perez *et al.*, 2016). Despite a lack of involvement in binding to GABA<sub>A</sub> receptors, there is considerable homology among loop G amino acids between  $\alpha$  subunits, consistent with a conserved role in receptor function (Fig. 1A).

The potential importance of loop G during gating is highlighted by comparisons of apo- and agonist bound structures of the glycine receptor (Du *et al.*, 2015) and GluCl (Althoff *et al.*, 2014). The  $\beta$ 1 strand containing loop G, the  $\beta$ 2 strand containing loop D and the interconnecting  $\beta$ 1- $\beta$ 2 loop, move towards the TM2-3 loop in the presence of bound agonist. This movement appears to precede the structural rearrangement of the TM domains that leads to channel opening (Calimet *et al.*, 2013).

We recently demonstrated the involvement of specific GABA<sub>A</sub> receptor  $\alpha$ 1 subunit loop G residues in function using cysteine-scanning mutagenesis (Baptista-Hon *et al.*, 2016). D43C was the only one of five loop G substituents to reduce the apparent potency of GABA. Furthermore, its modification by positively charged 2-aminoethyl methanethiosulfonate (MTSEA) caused additional functional impairment. By contrast, while T47C did not significantly affect GABA's potency, its modification by MTSEA inhibited GABA-evoked currents. Cysteines substituted at three other positions in loop G of the  $\alpha$ 1 subunit (residues 44, 45 and 46) were either inaccessible to MTSEA or their modification was without functional consequence (Baptista-Hon *et al.*, 2016).

In this study we investigated whether amino acid substitutions at positions 43 and 47 that impair function do so by impairing gating. In order to replicate MTSEA modified  $\alpha$ 1(T47C), which impairs function (Baptista-Hon *et al.*, 2016), we replaced Thr47 by Arg. We compared the efficacy of GABA as an activator of  $\alpha$ 1(D43C) $\beta$ 2 $\gamma$ 2,  $\alpha$ 1(T47R) $\beta$ 2 $\gamma$ 2 and  $\alpha$ 1 $\beta$ 2 $\gamma$ 2 receptors using analysis of channel open probability ( $P_{open}$ ) and potentiation by the positive allosteric modulator propofol. We investigated the kinetics of THIP- and propofol-evoked currents mediated by  $\alpha$ 1(T47R) $\beta$ 2 $\gamma$ 2 receptors. We also examined the influence of  $\alpha$ 1(T47R) substitution on receptors containing the  $\beta$ 2(L285R) substitution, which causes enhanced spontaneous gating. Using these approaches, we established that non-conservative substitutions at two key positions in loop G reduce gating efficacy.

## Methods

*Cell culture and transfection* - Human embryonic kidney 293 (HEK-293) cells were grown and maintained in Dulbecco Modified Eagle's Medium (DMEM) supplemented with 10% fetal bovine serum, 100  $\mu\text{g ml}^{-1}$  penicillin and 100 units  $\text{ml}^{-1}$  streptomycin at 37°C and 5%  $\text{CO}_2$ . Cells were seeded at low density in either poly-L-lysine coated, or uncoated 35 mm dishes for outside-out patch recordings or whole-cell recordings, respectively. Transfections were performed by calcium phosphate precipitation, using 1  $\mu\text{g}$  total cDNA per dish, as described previously (Baptista-Hon *et al.*, 2016). cDNAs encoding wild type (WT) and mutant mouse GABA<sub>A</sub> subunits were in the pRK5 mammalian expression vector. For heteromeric expression of GABA<sub>A</sub>  $\alpha 1\beta 2\gamma 2$  subunits, a 1:1:1 transfection ratio was used. cDNA encoding enhanced green fluorescence protein (in pEGFP vector, 0.1  $\mu\text{g}$ ) was included to identify successfully transfected cells using fluorescence microscopy. Transfected cells were functionally examined using voltage-clamp electrophysiology after 48 to 72 h. All tissue culture reagents were obtained from Invitrogen (Paisley, UK).

*Mutagenesis of GABA<sub>A</sub>  $\alpha 1$  and  $\beta 2$  subunits* – Single point mutations were performed by overlap extension polymerase chain reaction (PCR) (Heckman & Pease, 2007). For  $\alpha 1$  subunits, PCR products were digested using SmaI restriction endonuclease and EcoRI (5') and BamHI (3') restriction endonucleases were used for  $\beta 2$  subunits. All GABA<sub>A</sub> receptor subunits were ligated into pRK5 vector. All mutagenesis reactions and ligations were verified using agarose gel electrophoresis and sequenced prior to functional characterisation (Genetics Core Services, University of Dundee). All PCR and molecular cloning reagents were obtained from Fermentas (Thermo-Fisher, Loughborough, UK).

*Electrophysiology* - The whole-cell or excised outside-out patch configurations of the patch-clamp technique was used to record GABA-evoked currents from HEK-293 cells expressing WT, or mutant, GABA<sub>A</sub> receptors. Recording electrodes were fabricated from borosilicate glass capillaries, and when filled with intracellular solution had resistances of 1.3 – 2.3 M $\Omega$  for whole-cell recordings, and 3.0 – 5.0 M $\Omega$  for outside-out patch recordings. The electrode solution contained (in mM): 140 CsCl, 2 MgCl<sub>2</sub>, 1.1 EGTA, 3 Mg-ATP and 10 HEPES (pH 7.4 with CsOH). The extracellular solution contained (in mM): 140 NaCl, 4.7 KCl, 1.2 MgCl<sub>2</sub>, 2.5 CaCl<sub>2</sub>, 10 HEPES and 10 glucose (pH 7.4 with NaOH). Cells were voltage clamped at an electrode potential of -60 mV. For whole-cell recordings, currents were evoked by rapid application of agonists using the three-pipe Perfusion Fast Step system (Warner Instruments, CA, USA), as described previously (Baptista-Hon *et al.*, 2016).

For outside-out patch recordings, maximally efficacious and saturating concentrations of agonists were applied also using the Perfusion Fast Step system, with heat pulled and bevelled (Narashige, London, UK) theta and three-barrelled pipes (Othman et al., 2012). This allows rapid solution exchange consistently of <500  $\mu$ s around an open pipette tip (Hinkle & Macdonald, 2003). Solution exchange times were measured using liquid junction currents arising from moving the open pipette tip into an extracellular solution diluted by 10%. The 10-90% rise time of the liquid junction current was used as a measure of solution exchange rate. Liquid junction currents were routinely measured at the end of every outside-out patch recording, to ensure the fidelity of fast solution exchange. For experiments examining the macroscopic current kinetics of propofol-evoked currents, the concentration of propofol used was chosen on the basis that the evoked current does not contain a surge following propofol removal, which is mediated by propofol blockade (Hadley & Amin, 2007).

All electrophysiological data were recorded using an Axopatch 200B amplifier. Data were low pass filtered at 2 kHz for whole cell currents and 10 kHz for outside-out patch currents. Analog data were digitised at 20 kHz for whole cell currents and 100 kHz for outside-out patch currents using a Digidata 1320A interface and acquired using pCLAMP8 software (all from Molecular Devices, CA, USA).

*Data analysis* - The peak amplitudes of agonist-evoked currents were measured using Clampfit10 software (Molecular Devices, CA, USA), using averaged current traces from at least five agonist-evoked currents. The potentiating effects of propofol on peak GABA-evoked currents were analysed as percentage potentiation, using the formula:

$$\% \text{ potentiation} = \frac{(I_{pot} - I_{GABA})}{I_{GABA}} \times 100$$

Where  $I_{pot}$  and  $I_{GABA}$  represent the potentiated and control peak current amplitudes, respectively.

Non-stationary variance analysis was performed as described by Szczot et al (2014). A minimum of 10 consecutive responses to a 5 ms application of maximally efficacious and saturating concentration of GABA were recorded from outside-out patches, using the rapid application method described above. The currents were analysed using a custom-written script in MatLab (The Mathworks, Inc., Natick, Massachusetts, U.S.A.). The rising phase of each current was excluded from the analysis. The starting point for analysis was therefore set at the peak of the current. Mean current ( $I$ ) and variance ( $\sigma^2$ ) at each time point were divided into 30 equally spaced bins and plotted as  $I$  vs  $\sigma^2$ , which were fitted with the following function:



$$\sigma^2 = iI - I^2N^{-1} + C$$

Where  $i$  is the single channel amplitude,  $N$  is the number of channels and  $C$  is the background variance. From these parameters, the maximal open probability ( $P_{open}$ ) was calculated by:

$$\text{Maximal } P_{open} = \frac{\text{Peak } I}{i \times N}$$

Single channel conductance was calculated by dividing the single channel amplitude ( $i$ ) by the membrane holding potential (-60 mV).

Activation rates were measured using the 10 - 90% rise time of agonist-evoked inward current. Macroscopic desensitisation and deactivation kinetics were measured by fitting multi-exponential functions to the decaying phase of the inward current, during or following agonist application, respectively. The multi exponential function is defined by:

$$f(t) = A_1e^{-t/\tau_1} \dots + A_Ne^{-t/\tau_N}$$

Where  $\tau_N$  represent time constants and  $A_N$  represent the proportion of the particular  $\tau$ . The best-fit number of exponential terms (1 to 3 terms) were determined using an F-test with the confidence set at the 95% level. Rates of desensitisation and deactivation are provided as weighted  $\tau$  ( $\tau_w$ ) values, calculated using:

$$\tau_w = A_1 \times \tau_1 \dots + A_N \times \tau_N$$

Individual GABA concentration vs current amplitude relationships were fitted with a logistics equation:

$$f([GABA]) = \frac{100}{1 + 10^{(\log EC_{50} - [GABA]) \times n^H}}$$

From which GABA  $EC_{50}$  and Hill slope ( $n^H$ ) values were determined.

*Statistics* - Data are presented as mean  $\pm$  S.E.M. Differences in means of three or more groups were compared using one-way analysis of variance (ANOVA), with a *post-hoc* Dunnet's or Tukey's comparison. Pairwise comparisons were performed using the student t-test. In all cases  $P < 0.05$  was considered statistically significant. Statistical analyses were performed using GraphPad Prism 5 (GraphPad Software, San Diego, California, U.S.A.).

## Results

### *Residues in loop G and loop D influence the apparent potency of GABA*

Loop G of the GABA<sub>A</sub> receptor  $\alpha$  subunit contributes residues to the complimentary interface near the orthosteric binding site in heteropentameric GABA<sub>A</sub> receptors. The alignment reveals that the  $\alpha 1$  subunit Thr47 is entirely conserved among all GABA<sub>A</sub>  $\alpha$  subunits at the position equivalent to that of Arg37 in the *C. elegans* GluCl  $\alpha$  subunit (Fig. 1A). Asp43, an  $\alpha 1$  subunit residue we previously demonstrated to be important for GABA<sub>A</sub> receptor function (Baptista-Hon *et al.*, 2016) is also conserved in all but the  $\alpha 2$  subunit, which contains an Asn at the equivalent position. Loop G runs adjacent and anti-parallel to loop D on the  $\beta 2$  strand. The location of a critical loop D residue, Phe64, known to participate in GABA binding and efficacy is also shown in the alignment (Boileau *et al.*, 1999; Szczot *et al.*, 2014). Residues in these positions are highlighted on the GluCl structure in relation to bound glutamate (Fig. 1B) (Hibbs & Gouaux, 2011). GluCl Arg37 in loop G forms part of the glutamate binding site and is involved in receptor activation (Hibbs & Gouaux, 2011). We investigated the influence of the T47R substitution on GABA<sub>A</sub>  $\alpha 1\beta 2\gamma 2$  receptor function. Our previous study demonstrated that a non-conservative substitution to Asp43 (D43C) in loop G of the GABA<sub>A</sub>  $\alpha 1$  subunit significantly reduced the apparent potency of GABA (Baptista-Hon *et al.*, 2016).

WT  $\alpha 1$  or  $\alpha 1(T47R)$  subunits were transiently expressed with  $\beta 2$  and  $\gamma 2$  subunits in HEK-293 cells. Representative examples of GABA-evoked currents recorded under voltage-clamp at -60 mV from cells expressing  $\alpha 1\beta 2\gamma 2$  or  $\alpha 1(T47R)\beta 2\gamma 2$  receptors are shown in Figure 1C. GABA-evoked current amplitudes were expressed as a percentage of the maximum and plotted as a concentration-response relationship (Fig. 1D). A logistic function fitted to the data points reveals that the  $\alpha 1(T47R)$  substitution caused a rightward shift in the GABA concentration-response relationship (Fig 1D). The EC<sub>50</sub> for GABA activation of WT  $\alpha 1\beta 2\gamma 2$  receptors was  $17 \pm 5 \mu\text{M}$  ( $n = 7$ ). The EC<sub>50</sub> for GABA activation of  $\alpha 1(T47R)\beta 2\gamma 2$  receptors was  $1500 \pm 320 \mu\text{M}$  ( $n = 7$ ). The non-conservative D43C substitution in loop G of the GABA<sub>A</sub>  $\alpha 1$  subunit produced a similar reduction in the apparent potency of GABA (Baptista-Hon *et al.*, 2016).

Phe64, which is located on the adjacent and anti-parallel loop D is involved in GABA binding and gating (Boileau *et al.*, 1999; Szczot *et al.*, 2014). The  $\alpha 1(F64C)$  substitution causes a significant reduction in the apparent potency of GABA (Boileau *et al.*, 1999; Szczot *et al.*, 2014; Baptista-Hon *et al.*, 2016). Substitution of Phe64 with the equivalent residue found at this position in GluCl (F64T) caused a similar impairment in the apparent potency of GABA. The EC<sub>50</sub> of  $\alpha 1(F64T)\beta 2\gamma 2$  receptors was  $16 \pm 1 \text{ mM}$  ( $n = 3$ ). A one-way ANOVA revealed a significant difference between the GABA EC<sub>50</sub>

values ( $P < 0.0001$ ). A *post-hoc* Tukey's comparison revealed statistically significant differences in GABA  $EC_{50}$  between WT and  $\alpha 1(T47R)\beta 2\gamma 2$  receptors ( $P < 0.05$ ), between WT and  $\alpha 1(F64T)\beta 2\gamma 2$  receptors ( $P < 0.0001$ ) and also between  $\alpha 1(T47R)\beta 2\gamma 2$  and  $\alpha 1(F64T)\beta 2\gamma 2$  receptors ( $P < 0.0001$ ). There were no statistically significant differences in the Hill slope values of the GABA concentration-response relationships ( $P = 0.24$ ; one-way ANOVA). This observation suggests that the number of GABA binding sites remains the same and argues against altered stoichiometry caused by the  $\alpha 1$  subunit substitutions. We also evaluated the peak current density of  $\alpha 1\beta 2\gamma 2$ ,  $\alpha 1(T47R)\beta 2\gamma 2$  and  $\alpha 1(F64T)\beta 2\gamma 2$  receptors, by normalising the current amplitude evoked by maximally efficacious concentrations of GABA, to cell capacitances. The mean ( $\pm$  S.E.M.) current densities are  $1510 \pm 264$  pA  $pF^{-1}$  ( $n = 18$ ),  $684 \pm 119$  pA  $pF^{-1}$  ( $n = 24$ ) and  $401 \pm 155$  pA  $pF^{-1}$  ( $n = 5$ ), for  $\alpha 1\beta 2\gamma 2$ ,  $\alpha 1(T47R)\beta 2\gamma 2$  and  $\alpha 1(F64T)\beta 2\gamma 2$  receptors, respectively. There was a statistically significant difference in peak current density ( $P = 0.003$ ; one-way ANOVA). A *post-hoc* Tukey's comparison revealed significant reductions in the mean current densities for  $\alpha 1(T47R)\beta 2\gamma 2$  ( $P < 0.001$ ), and  $\alpha 1(F64T)\beta 2\gamma 2$  receptors ( $P < 0.05$ ), when compared with  $\alpha 1\beta 2\gamma 2$  receptors. We have previously reported a reduction in current density for  $\alpha 1(D43C)\beta 2\gamma 2$  and  $\alpha 1(F64C)\beta 2\gamma 2$  receptors, compared to WT receptors (Baptista-Hon *et al.*, 2016).

#### *The identities of residues in Loop G at positions 43 and 47 influence agonist efficacy*

Apparent potencies, determined from concentration-response relationships, are composites of agonist binding affinity and gating efficacy (Colquhoun, 1998). Therefore, reductions in  $EC_{50}$  values for  $\alpha 1(D43C)\beta 2\gamma 2$  and  $\alpha 1(T47R)\beta 2\gamma 2$  receptors compared to WT could be caused by reduced GABA affinity and/or efficacy. We investigated the possibility that D43C and T47R substitutions might impair the efficacy of GABA using propofol, a general anaesthetic that acts as a positive allosteric modulator of GABA<sub>A</sub> receptors (Berger *et al.*, 1997). Co-application of propofol (1  $\mu$ M) with an  $EC_{50}$  concentration of GABA (10  $\mu$ M) to HEK-293 cells expressing  $\alpha 1\beta 2\gamma 2$  receptors caused current amplitudes to increase by  $62 \pm 18\%$  ( $n = 4$ ), relative to currents evoked by GABA (10  $\mu$ M) alone. The application of propofol (1  $\mu$ M) alone had no effect (data not shown). We subsequently tested the ability of propofol (1  $\mu$ M) to potentiate currents evoked by maximally efficacious concentrations of GABA mediated by  $\alpha 1\beta 2\gamma 2$  (1 mM),  $\alpha 1(D43C)\beta 2\gamma 2$  (100 mM),  $\alpha 1(T47R)\beta 2\gamma 2$  (30 mM) and  $\alpha 1(F64C)\beta 2\gamma 2$  receptors (300 mM). GABA concentrations were chosen based on the concentration-response relationship shown in Figure 1D for  $\alpha 1\beta 2\gamma 2$  and  $\alpha 1(T47R)\beta 2\gamma 2$  receptors, and our previously published concentration-response relationships for  $\alpha 1(D43C)\beta 2\gamma 2$  and  $\alpha 1(F64C)\beta 2\gamma 2$  receptors (Baptista-Hon *et al.*, 2016). Figure 2A shows representative examples of maximal GABA-evoked currents in the presence or absence of propofol. Co-application of propofol with GABA to

cells expressing  $\alpha 1\beta 2\gamma 2$  receptors did not cause any potentiation, consistent with GABA having full efficacy. By contrast, recordings from cells expressing  $\alpha 1(D43C)\beta 2\gamma 2$  or  $\alpha 1(T47R)\beta 2\gamma 2$  receptors revealed that the co-application of GABA with propofol increased current amplitudes relative to GABA alone (Fig. 2A). This suggests that GABA lacks full efficacy at  $\alpha 1(D43C)\beta 2\gamma 2$  and  $\alpha 1(T47R)\beta 2\gamma 2$  receptors. The loop D  $\alpha 1(F64C)$  substitution is known to reduce the efficacy of GABA (Szczo $t et al.$ , 2014). Consistent with this observation, we found that co-application of GABA (300 mM) with propofol (1  $\mu$ M) also increased the current amplitude relative to GABA (300 mM) alone at  $\alpha 1(F64C)\beta 2\gamma 2$  receptors (Fig. 2A). We quantified the effect of propofol on maximal GABA-evoked currents (Fig. 2B). The graph shows data expressed as mean percent potentiation by propofol. Currents mediated by  $\alpha 1\beta 2\gamma 2$  receptors were unaffected by propofol ( $-0.72 \pm 1.6\%$ ;  $n = 5$ ). By contrast, propofol (1  $\mu$ M) potentiated maximal GABA-evoked currents mediated by  $\alpha 1(D43C)\beta 2\gamma 2$ ,  $\alpha 1(T47R)\beta 2\gamma 2$  and  $\alpha 1(F64C)\beta 2\gamma 2$  receptors by  $19 \pm 5\%$  ( $n = 9$ ),  $23 \pm 5\%$  ( $n = 9$ ) and  $47 \pm 8\%$  ( $n = 4$ ), respectively (Fig. 2B). The differences in mean percentage potentiation were statistically significant ( $P < 0.0001$ ; one-way ANOVA). A *post-hoc* Tukey's comparison revealed a statistically significant difference in propofol potentiation of maximal GABA-evoked currents between  $\alpha 1\beta 2\gamma 2$  and  $\alpha 1(D43C)\beta 2\gamma 2$  ( $P < 0.05$ ),  $\alpha 1(T47R)\beta 2\gamma 2$  ( $P < 0.001$ ) and  $\alpha 1(F64C)\beta 2\gamma 2$  receptors ( $P < 0.0001$ ). There is also a significant difference in propofol potentiation between  $\alpha 1(F64C)\beta 2\gamma 2$  and either  $\alpha 1(D43C)\beta 2\gamma 2$  ( $P < 0.001$ ) or  $\alpha 1(T47R)\beta 2\gamma 2$  receptors ( $P < 0.05$ ). These data indicate that D43C and T47R substitutions impair the efficacy of GABA, albeit to a lesser extent than the F64C substitution.

We examined whether the reduced efficacy of GABA as an agonist at  $\alpha 1(D43C)\beta 2\gamma 2$  or  $\alpha 1(T47R)\beta 2\gamma 2$  was associated with reduced maximal open probabilities ( $P_{open}$ ) of GABA-activated channels as would be expected for mutations that affect gating. We calculated  $P_{open}$  using non-stationary variance analysis of maximal GABA-evoked currents. This approach has been used previously to demonstrate that the  $P_{open}$  of GABA $_A$  receptors containing the  $\alpha 1(F64C)$  substitution was reduced (Szczo $t et al.$ , 2014). Currents evoked by brief (5 ms) rapid applications of maximally efficacious concentrations of GABA were recorded from outside-out patches containing  $\alpha 1\beta 2\gamma 2$ ,  $\alpha 1(D43C)\beta 2\gamma 2$  or  $\alpha 1(T47R)\beta 2\gamma 2$  receptors. A minimum of 10 consecutive GABA-evoked currents were used to calculate mean current ( $I$ ) and variance ( $\sigma^2$ ) for each time point. Representative examples of variance and mean current are shown for  $\alpha 1\beta 2\gamma 2$  and  $\alpha 1(T47R)\beta 2\gamma 2$  receptors (Fig. 3A). The rising phases of the currents were not included in the analysis (grey portion in Fig. 3A). A parabolic function was fitted to the plot of mean current versus variance to determine the single channel amplitude and the number of channels (Fig. 3B). From these values, the single channel conductance ( $\gamma$ ) and maximal  $P_{open}$  were calculated (See Methods). Neither the  $\alpha 1(D43C)$  nor

$\alpha 1(T47R)$  substitutions significantly altered  $\gamma$  (Fig. 3C;  $P = 0.96$ ; one-way ANOVA). The mean maximum  $P_{open}$  values for  $\alpha 1\beta 2\gamma 2$ ,  $\alpha 1(D43C)\beta 2\gamma 2$  and  $\alpha 1(T47R)\beta 2\gamma 2$  receptors were  $0.78 \pm 0.05$  ( $n = 8$ ),  $0.50 \pm 0.09$  ( $n = 5$ ) and  $0.56 \pm 0.05$  ( $n = 7$ ), respectively (Fig. 3D). One-way ANOVA revealed a statistically significant difference in mean maximal  $P_{open}$  ( $P = 0.0083$ ). A *post-hoc* Tukey's comparison determined a statistically significant difference in mean maximal  $P_{open}$  between  $\alpha 1\beta 2\gamma 2$  and  $\alpha 1(D43C)\beta 2\gamma 2$  receptors ( $P < 0.05$ ), and between  $\alpha 1\beta 2\gamma 2$  and  $\alpha 1(T47R)\beta 2\gamma 2$  receptors ( $P < 0.05$ ). These data agree well with the results of propofol potentiation experiments and indicate that the  $\alpha 1(D43C)$  and  $\alpha 1(T47R)$  substitutions reduce the efficacy of GABA by reducing the maximal  $P_{open}$  of  $GABA_A$  receptors to a similar extent.

#### *Substitutions in loop G and loop D have common effects on GABA-evoked gating kinetics*

We used rapid GABA application to outside-out patches excised from HEK-293 cells to investigate the kinetics of macroscopic currents mediated by recombinant  $\alpha 1(D43C)\beta 2\gamma 2$ ,  $\alpha 1(T47R)\beta 2\gamma 2$  and  $\alpha 1(F64C)\beta 2\gamma 2$  receptors. Figure 4A shows representative examples of currents evoked by maximal concentrations of GABA, recorded at  $-60$  mV from patches containing  $\alpha 1\beta 2\gamma 2$ ,  $\alpha 1(D43C)\beta 2\gamma 2$ ,  $\alpha 1(T47R)\beta 2\gamma 2$  and  $\alpha 1(F64C)\beta 2\gamma 2$  receptors. Macroscopic currents mediated by  $\alpha 1(F64T)\beta 2\gamma 2$  receptors resemble those of  $\alpha 1(F64C)\beta 2\gamma 2$  receptors and are not shown. Traces in Figure 4B are amplitude-normalised rising phases mediated by  $\alpha 1\beta 2\gamma 2$ ,  $\alpha 1(T47R)\beta 2\gamma 2$  and  $\alpha 1(F64C)\beta 2\gamma 2$  receptors. Current activation rates were quantified as 10 - 90% rise-times. Mean activation times are plotted in the bar graph (Fig. 4B). Comparison of the mean rise-times reveals a statistically significant difference between these receptor subtypes ( $P < 0.0001$ ; one-way ANOVA; Fig. 4B; Table 1). Currents mediated by both  $\alpha 1(F64C)\beta 2\gamma 2$  and  $\alpha 1(F64T)\beta 2\gamma 2$  receptors were activated more slowly than  $\alpha 1\beta 2\gamma 2$  ( $P < 0.0001$ ) and also when compared with  $\alpha 1(D43C)\beta 2\gamma 2$  ( $P < 0.0001$ ) and  $\alpha 1(T47R)\beta 2\gamma 2$  receptors ( $P < 0.0001$ , *post-hoc* Tukey's comparison). The activation rates between  $\alpha 1\beta 2\gamma 2$ ,  $\alpha 1(D43C)\beta 2\gamma 2$  and  $\alpha 1(T47R)\beta 2\gamma 2$  receptors did not differ significantly. However, there was a trend towards a slower activation rate for both loop G substitutions.

GABA-evoked currents decay in the continued presence of the agonist through the process of desensitisation. We quantified desensitisation by measuring current remaining at the end of the GABA application and expressing it as a percentage of peak current amplitude. The averaged values are plotted in Figure 4C. Comparison of these values reveals a significant difference between the receptor subtypes ( $P = 0.0003$ ; one-way ANOVA; Fig. 4C). GABA-evoked currents mediated by  $\alpha 1(D43C)\beta 2\gamma 2$ ,  $\alpha 1(F64C)\beta 2\gamma 2$  and  $\alpha 1(F64T)\beta 2\gamma 2$  receptors desensitised significantly less than those

mediated by  $\alpha 1\beta 2\gamma 2$  receptors ( $P < 0.001$ , *post-hoc* Tukey's comparison). The extent of desensitisation did not significantly differ between  $\alpha 1\beta 2\gamma 2$  and  $\alpha 1(T47R)\beta 2\gamma 2$  receptors.

It was possible to fit exponential functions to evaluate the apparent desensitisation rates for  $\alpha 1\beta 2\gamma 2$ ,  $\alpha 1(D43C)\beta 2\gamma 2$  and  $\alpha 1(T47R)\beta 2\gamma 2$  receptors. An F-test (see Methods) revealed that a three-component exponential function consistently yielded the best fit to the desensitising current. The components of the multi-exponential function were used to calculate  $\tau_w$  (see Methods) and the mean values of  $\tau_w$  are plotted in Figure 4D. There was no significant difference in mean  $\tau_w$  values ( $P = 0.08$ ; one-way ANOVA), although visual inspection of the exemplar traces in Figure 4A shows apparent differences in the time course of desensitisation between  $\alpha 1\beta 2\gamma 2$ ,  $\alpha 1(D43C)\beta 2\gamma 2$  and  $\alpha 1(T47R)\beta 2\gamma 2$  receptors. Indeed, analysis of the individual components of desensitisation reveals significant differences (Table 1). The  $\alpha 1(D43C)$  and  $\alpha 1(T47R)$  substitutions influence the fastest component of apparent desensitisation by reducing the rate and the percentage, respectively. There was also an increase in the contribution of the slowest time constant to apparent desensitisation for  $\alpha 1(D43C)\beta 2\gamma 2$  and  $\alpha 1(T47R)\beta 2\gamma 2$  receptors. The intermediate component was not affected by the substitutions. These analyses indicate that the loop G  $\alpha 1(D43C)$  and  $\alpha 1(T47R)$  substitutions cause similar changes in desensitisation kinetics.

Traces in Figure 4E show amplitude normalised deactivation time courses of  $\alpha 1\beta 2\gamma 2$ ,  $\alpha 1(T47R)\beta 2\gamma 2$  and  $\alpha 1(F64C)\beta 2\gamma 2$  receptors. The deactivation traces for  $\alpha 1(D43C)\beta 2\gamma 2$ ,  $\alpha 1(T47R)\beta 2\gamma 2$ ,  $\alpha 1(F64C)\beta 2\gamma 2$  and  $\alpha 1(F64T)\beta 2\gamma 2$  receptors are indistinguishable from each other. Therefore, for clarity, examples of  $\alpha 1(D43C)\beta 2\gamma 2$  and  $\alpha 1(F64T)\beta 2\gamma 2$  receptors are not shown. An F-test revealed that a three-component exponential function best describes the deactivation time course in  $\alpha 1\beta 2\gamma 2$ ,  $\alpha 1(D43C)\beta 2\gamma 2$  and  $\alpha 1(T47R)\beta 2\gamma 2$  receptors. For  $\alpha 1(F64C)\beta 2\gamma 2$  and  $\alpha 1(F64T)\beta 2\gamma 2$  receptors, the slowest component was lost and the deactivation time courses were best described with a two-exponential function. Comparison of the mean  $\tau_w$  values for deactivation of GABA-evoked currents mediated by the different receptor subtypes revealed a statistically significant difference ( $P < 0.0001$ ; one-way ANOVA; Fig. 4E; Table 2). There were significant differences between the  $\tau_w$  values for  $\alpha 1\beta 2\gamma 2$  and  $\alpha 1(D43C)\beta 2\gamma 2$ ,  $\alpha 1(T47R)\beta 2\gamma 2$ ,  $\alpha 1(F64C)\beta 2\gamma 2$  and  $\alpha 1(F64T)\beta 2\gamma 2$  receptors (all  $P < 0.0001$ , *post-hoc* Tukey's comparison). The individual components of the multi-exponential fits are summarised in Table 2. Macroscopic currents mediated by GABA<sub>A</sub> receptors containing the loop D  $\alpha 1(F64C)$  and  $\alpha 1(F64T)$  substitutions were more severely affected, in terms of activation rates and extent of apparent desensitisation, than were those containing the  $\alpha 1(D43C)$  and  $\alpha 1(T47R)$  substitutions. By contrast, deactivation rates were similarly affected by all substitutions in loops G and D.

*Kinetics of currents activated by the partial agonist THIP*

In the preceding investigation of GABA efficacy and gating kinetics, the loop G  $\alpha 1$ (D43C) and  $\alpha 1$ (T47R) substitutions had similar effects. We therefore restricted our subsequent analysis to the  $\alpha 1$ (T47R) substitution using the loop D  $\alpha 1$ (F64C) substitution as a comparator.

Propofol potentiation and maximal  $P_{open}$  data suggest that the efficacy of GABA is impaired by non-conservative substitutions in loop G. These changes in efficacy were associated with dramatically increased deactivation rates and changes in desensitisation kinetics. We investigated currents evoked by THIP, a partial agonist at WT GABA<sub>A</sub>  $\alpha 1\beta 2\gamma 2$  receptors to determine whether these are kinetic hallmarks of partial agonism.

We verified that THIP is a partial agonist when applied rapidly (see Methods) to excised outside-out patches containing  $\alpha 1\beta 2\gamma 2$  receptors. Maximally effective concentrations of GABA and THIP were chosen on the basis of concentration-response relationships (Fig. 1D) and the observation that higher agonist concentrations did not further increase current amplitude when applied rapidly to outside-out patches (data not shown). Figure 5A shows representative examples of maximally effective GABA- and THIP-evoked currents recorded from outside-out patches containing  $\alpha 1\beta 2\gamma 2$  and  $\alpha 1$ (T47R) $\beta 2\gamma 2$  receptors. THIP-evoked currents mediated by  $\alpha 1\beta 2\gamma 2$  receptors were smaller than those activated by GABA (Fig. 5B). The exemplar data reveal a further reduction in the relative THIP-evoked current amplitude mediated by  $\alpha 1$ (T47R) $\beta 2\gamma 2$  receptors, consistent with our data above that this non-conservative substitution reduces agonist efficacy. THIP did not evoke measurable currents at  $\alpha 1$ (F64C) $\beta 2\gamma 2$  receptors (data not shown). The relative efficacy of THIP at  $\alpha 1\beta 2\gamma 2$  receptors, was on average  $77 \pm 5\%$  of that of GABA ( $n = 5$ ; Fig. 5B). The relative efficacy of THIP as an agonist of  $\alpha 1$ (T47R) $\beta 2\gamma 2$  receptors was reduced to  $17 \pm 3\%$  of that of GABA ( $n = 6$ ). The reduction in THIP efficacy at  $\alpha 1$ (T47R) $\beta 2\gamma 2$  receptors was statistically significant ( $P = 0.0001$ ; t-test; Fig. 5B).

Inspection of  $\alpha 1\beta 2\gamma 2$  receptor-mediated currents reveals that those activated by THIP and GABA exhibit differing kinetics (Fig. 5A). The normalised current traces in Figure 5C illustrate the rising phases of GABA- and THIP-evoked currents mediated by WT receptors. We compared their activation rates by measuring the time for currents to increase from 10% to 90% of their peaks (Fig. 5C). THIP-evoked currents activated significantly more slowly than did GABA-evoked currents ( $P < 0.0001$ ; t-test).

The apparent desensitisation time course for THIP-evoked currents mediated by  $\alpha 1\beta 2\gamma 2$  receptors was best described using a three-component exponential function. THIP-evoked currents showed subtle differences in desensitisation kinetics compared with GABA-evoked currents. There was no statistically significant difference in the  $\tau_w$  between GABA-evoked and THIP-evoked currents (Fig. 5D;  $P = 0.29$ ; t-test). The individual time constants and their relative proportions are summarised in Table 1. There was a significant reduction in the proportion of the fastest desensitisation component, and a concurrent significant increase in the slowest component. The effect of a partial agonist on desensitisation time course at  $\alpha 1\beta 2\gamma 2$  receptors is similar to those caused by the loop G  $\alpha 1(D43C)$  and  $\alpha 1(T47R)$  substitutions, which impaired efficacy.

Traces in Figure 5E (normalised to the amplitude at the end of a 500 ms GABA application) are examples of GABA- and THIP-evoked current deactivation mediated by WT receptors. The deactivation time course for THIP-evoked currents were best described using a triple exponential function, similar to GABA-evoked currents. Comparison of mean  $\tau_w$  values reveal that THIP-evoked currents deactivate significantly faster than GABA-evoked currents ( $P = 0.0008$ , t-test; Fig. 5E). The individual components of the deactivation kinetics are summarised in Table 2. The increase in the  $\tau_w$  of deactivation can be attributed to a significant reduction in all three time constants and a shift in the proportion from the slowest to the fastest component. These data agree well with our findings above that partial agonism is associated with an increase in deactivation rate, but also, to a lesser extent, with slower activation and desensitisation kinetics. These findings support a previous report of kinetics associated with partial efficacy using single channel recording (Mortensen et al., 2004) and imply that slow activation, slow desensitisation and fast deactivation are associated with weaker agonists.

In the presence of the  $\alpha 1(T47R)$  substitution, the efficacy of THIP is further reduced relative to GABA (Fig. 5A). We therefore compared the macroscopic kinetics of THIP-evoked currents mediated by  $\alpha 1\beta 2\gamma 2$  and  $\alpha 1(T47R)\beta 2\gamma 2$  receptors. The current traces in Figure 5F show amplitude normalised rising phases of THIP-evoked currents mediated by  $\alpha 1\beta 2\gamma 2$  and  $\alpha 1(T47R)\beta 2\gamma 2$  receptors. The bar graph shows mean 10 - 90% rise times. THIP-evoked currents mediated by  $\alpha 1(T47R)\beta 2\gamma 2$  receptors were activated significantly more slowly than those mediated by  $\alpha 1\beta 2\gamma 2$  receptors ( $P = 0.002$ ; t-test; Fig. 5F; Table 1).

Currents mediated by  $\alpha 1(T47R)\beta 2\gamma 2$  receptors desensitised too slowly to allow fitting with an exponential function (see Fig. 5A). Therefore, we examined desensitisation by measuring the current remaining at the end of the THIP application as a percentage of that at its peak. This approach



revealed a significant reduction in the extent of THIP-evoked current desensitisation mediated by  $\alpha 1(T47R)\beta 2\gamma 2$  receptors compared to those mediated by  $\alpha 1\beta 2\gamma 2$  receptors ( $P = 0.0001$ ; t-test; Fig. 5G; Table 1).

The current traces in Figure 5H show amplitude normalised deactivation phases from THIP-evoked currents at  $\alpha 1\beta 2\gamma 2$  and  $\alpha 1(T47R)\beta 2\gamma 2$  receptors. The deactivation of THIP-evoked currents mediated by  $\alpha 1(T47R)\beta 2\gamma 2$  receptors was consistently best described using two exponential terms, compared to three terms necessary to adequately describe deactivation mediated by  $\alpha 1\beta 2\gamma 2$  receptors. Analysis of the mean  $\tau_w$  values reveals a significant reduction of the  $\tau_w$  values for the activation of THIP-evoked currents mediated by  $\alpha 1(T47R)\beta 2\gamma 2$  receptors compared to WT receptors ( $P = 0.0001$ ; t-test; Fig. 3G; Table 2). There was a significant reduction in the fastest time constant, as well as a significant increase in its proportion. As mentioned above, the slowest deactivation time constant present in recordings of THIP-evoked currents mediated by WT receptors were not seen in recording of currents mediated by  $\alpha 1(T47R)\beta 2\gamma 2$  receptors. These data agree well with the other macroscopic current kinetic data showing progressively increasing effects on activation and deactivation rates with reductions in agonist efficacy.

#### *Deactivation kinetics of propofol-evoked currents*

It is possible that the changes in current kinetics quantified above (slow activation, slow desensitisation and fast deactivation), caused by mutations in the vicinity of the orthosteric binding site are composites of altered rates of agonist association and dissociation, agonist efficacy and desensitisation. This might be expected particularly for the  $\alpha 1(F64C)$  mutation, which affects agonist binding. In order to examine the effect of amino acid substitutions in loop G and loop D on receptor gating, independent of orthosteric agonist binding we examined the kinetics of currents activated by the allosteric agonist propofol mediated by  $\alpha 1\beta 2\gamma 2$ ,  $\alpha 1(T47R)\beta 2\gamma 2$  and  $\alpha 1(F64C)\beta 2\gamma 2$  receptors. The concentration of propofol used, which evoked robust currents without evidence of block, was either 30 or 100  $\mu M$ , and did not differ between the receptor subtypes, suggesting that the potency for propofol was not dramatically affected by the amino acid substitutions. The activation time course of propofol (30 or 100  $\mu M$ )-evoked currents mediated by  $\alpha 1\beta 2\gamma 2$  receptors, was independent of concentration (data not shown).

Figure 6A shows representative examples of propofol-evoked currents recorded from outside-out patches containing  $\alpha 1\beta 2\gamma 2$ ,  $\alpha 1(T47R)\beta 2\gamma 2$  and  $\alpha 1(F64C)\beta 2\gamma 2$  receptors. The current traces in Figure 6B are amplitude normalised rising phases of propofol-evoked currents mediated by WT and mutant receptors. We measured activation rate as the 10 - 90% rise time. The means are plotted in the bar

graph (Fig. 6B). The  $\alpha 1(T47R)$  and  $\alpha 1(F64C)$  substitutions did not significantly affect the 10 - 90% rise time of propofol-evoked currents ( $P = 0.51$ ; one-way ANOVA).

Propofol (30 or 100  $\mu M$ )-evoked currents did not exhibit measurable apparent desensitisation and therefore this parameter was not analysed (Fig. 6A). Traces in Figure 6C are amplitude normalised deactivation phases of propofol-evoked currents mediated by  $\alpha 1\beta 2\gamma 2$ ,  $\alpha 1(T47R)\beta 2\gamma 2$  and  $\alpha 1(F64C)\beta 2\gamma 2$  receptors. A double exponential best describes the deactivation time course and the mean  $\tau_w$  is plotted in the bar graph (Fig. 6C). Comparison of the  $\tau_w$  values for deactivation revealed a significant differences (one-way ANOVA) between  $\alpha 1\beta 2\gamma 2$ ,  $\alpha 1(T47R)\beta 2\gamma 2$  ( $P < 0.0001$ ) and  $\alpha 1(F64C)\beta 2\gamma 2$  ( $P < 0.0001$ , *post-hoc* Tukey's comparison). The  $\tau_w$  of deactivation did not differ between different mutant receptors. These data demonstrate that the deactivation rate for the allosteric agonist propofol is affected by the T47R and F64C substitutions, suggesting that loop D Phe64 and loop G Thr47 are involved in gating of  $\alpha 1\beta 2\gamma 2$  GABA<sub>A</sub> receptors independent of occupation of the orthosteric binding site.

#### *$\alpha 1$ subunit T47R reduces spontaneous gating*

Our observation that propofol-evoked currents were influenced by the  $\alpha 1(T47R)$  substitution suggests that loop G Thr47 influences gating regardless of the occupancy of the orthosteric binding site. In order to examine the influence of the  $\alpha 1(T47R)$  and  $\alpha 1(F64C)$  substitutions on GABA<sub>A</sub> receptor gating independent of any agonist activation, we studied their effects on GABA<sub>A</sub> receptors that display enhanced spontaneous gating. Leu285 is a conserved residue in all  $\beta$ -subunits located in TM3. The GABA<sub>A</sub>  $\beta 1(L285R)$  substitution is associated with alcohol preference and enhanced spontaneous gating (Anstee *et al.*, 2013).

We first determined whether GABA<sub>A</sub>  $\alpha 1\beta 2(L285R)\gamma 2$  receptors also displayed enhanced spontaneous gating by applying picrotoxin (100  $\mu M$ ) to block spontaneous currents recorded in the absence of agonist ( $I_{spont}$ ). Maximal GABA evoked currents ( $I_{GABA}$ ) were then recorded. We quantified the extent of spontaneous gating as the percentage of  $I_{spont}$  to  $I_{GABA}$  ( $I_{spont}/I_{GABA}$ ). The  $\beta 2(L285R)$  substitution conferred enhanced  $I_{spont}$  (Fig. 7). We investigated the effect of the  $\alpha 1(T47R)$  and  $\alpha 1(F64C)$  substitutions on these currents. However, GABA failed to activate  $\alpha 1(F64C)\beta 2(L285R)\gamma 2$  receptors, while picrotoxin inhibited standing currents ( $n = 3$ ; data not shown). Therefore our subsequent experiments were restricted to the  $\alpha 1(T47R)$  substitution. Figure 7A shows representative examples of  $I_{spont}$  (grey traces) and  $I_{GABA}$  (black traces) mediated by  $\alpha 1\beta 2\gamma 2$ ,  $\alpha 1\beta 2(L285R)\gamma 2$  and  $\alpha 1(T47R)\beta 2(L285R)\gamma 2$  receptors. The presence of the  $\alpha 1(T47R)$  substitution reduced the amplitude of  $I_{spont}$  relative to  $I_{GABA}$  (Fig. 7A). The mean extent of spontaneous gating is plotted in Figure 7B. WT

$\alpha 1\beta 2\gamma 2$  receptors had negligible  $I_{\text{spont}}/I_{\text{GABA}}$  ( $0.0008 \pm 0.0002\%$ ;  $n = 6$ ). By contrast,  $\alpha 1\beta 2(\text{L285R})\gamma 2$  receptors had enhanced  $I_{\text{spont}}/I_{\text{GABA}}$  ( $65 \pm 12\%$ ;  $n = 4$ ) and that of  $\alpha 1(\text{T47R})\beta 2(\text{L285R})\gamma 2$  receptors was only  $12 \pm 5\%$  ( $n = 4$ ). A one-way ANOVA revealed a statistically significant difference in mean  $I_{\text{spont}}/I_{\text{GABA}}$  ( $P < 0.0001$ ). A *post-hoc* Tukey's comparison revealed statistically significant differences between the mean  $I_{\text{spont}}/I_{\text{GABA}}$  of  $\alpha 1\beta 2\gamma 2$  and  $\alpha 1\beta 2(\text{L285R})\gamma 2$  receptors ( $P < 0.0001$ ), and between  $\alpha 1\beta 2(\text{L285R})\gamma 2$  and  $\alpha 1(\text{T47R})\beta 2(\text{L285R})\gamma 2$  receptors ( $P < 0.0001$ ). Our data therefore demonstrate that the  $\beta 2(\text{L285R})$  substitution confers greatly enhanced spontaneous activity, but the  $\alpha 1(\text{T47R})$  substitution attenuated this effect. This demonstrates that the  $\alpha 1(\text{T47R})$  substitution reduces the gating of  $\text{GABA}_A$   $\alpha 1\beta 2\gamma 2$  receptors independent of any agonist occupancy.

## Discussion

Data from this study and our previous study respectively demonstrate that two substitutions, T47R and D43C, at strategic locations in loop G reduce the apparent potency of GABA (Baptista-Hon *et al.*, 2016). Changes in apparent potency can be caused by reduced binding affinity and/or gating efficacy (Colquhoun, 1998). Both mechanisms contribute to the reduced apparent potency of GABA caused by the  $\alpha 1$ (F64C) loop D substitution (Szcot *et al.*, 2014; Baptista-Hon *et al.*, 2016). Loop D located in the  $\beta 2$  strand is critical for agonist binding in the GABA<sub>A</sub> receptor and, consistent with this, modification of Cys64 by MTSEA is hindered by GABA, but not by the allosteric agonists, propofol and pentobarbital (Holden & Czajkowski, 2002; Baptista-Hon *et al.*, 2016). By contrast, we previously demonstrated that both GABA and propofol reduce the rate of MTSEA modification of Cys43 and Cys47 in  $\alpha 1$ (D43C) $\beta 2\gamma 2$  and  $\alpha 1$ (T47C) $\beta 2\gamma 2$  receptors, respectively (Baptista-Hon *et al.*, 2016). This is consistent with movement associated with gating being the cause of reduced accessibility, rather than agonist binding. Movement of loop G during gating may be responsible for reduced accessibility to MTSEA. Furthermore, restriction of movement by non-conservative substitutions of amino acids at positions 43 and 47 may impair gating leading to the observed dextral shift in the GABA concentration-response relationship for  $\alpha 1$ (D43C) $\beta 2\gamma 2$  and  $\alpha 1$ (T47R) $\beta 2\gamma 2$  receptors relative to WT.

We directly explored whether the  $\alpha 1$ (D43C) and  $\alpha 1$ (T47R) substitutions reduce GABA efficacy using propofol at a concentration below that required for activation, but sufficient for positive allosteric modulation of sub-maximal GABA-evoked currents mediated by WT receptors (Berger *et al.*, 1997). Propofol potentiated maximal GABA-evoked currents mediated by both  $\alpha 1$ (D43C) $\beta 2\gamma 2$  and  $\alpha 1$ (T47R) $\beta 2\gamma 2$ , but not WT receptors. This suggests that propofol restores the efficacy of GABA lost through the D43C and T47R substitutions in loop G. Using non-stationary variance analysis, we also demonstrated that the maximal  $P_{open}$  is reduced for  $\alpha 1$ (D43C) $\beta 2\gamma 2$  and  $\alpha 1$ (T47R) $\beta 2\gamma 2$  receptors, without a change in single channel conductance, indicating that loop G does indeed play a role in efficacy. Using the same approach, it was demonstrated that the loop D  $\alpha 1$ (F64C) substitution also reduces maximal  $P_{open}$ , albeit to a greater extent (Szcot *et al.*, 2014). Our data showing that the magnitude of propofol potentiation of a maximally efficacious concentration of GABA was greater in  $\alpha 1$ (F64C) $\beta 2\gamma 2$  receptors, than in  $\alpha 1$ (D43C) $\beta 2\gamma 2$  and  $\alpha 1$ (T47R) $\beta 2\gamma 2$  receptors agrees well with the relative impairments of  $P_{open}$  associated with these substitutions. Furthermore, the efficacy of THIP was also reduced by loop G and loop D substitutions providing additional evidence that orthosteric agonist efficacy is indeed impaired.

Mounting structural evidence suggests that the antiparallel  $\beta 1$  and  $\beta 2$  strands, which contain loop G and loop D, respectively, move during gating. Comparisons of apo- and ligand-bound structures of the glycine receptor (Du *et al.*, 2015), and the *C. elegans* GluCl (Althoff *et al.*, 2014) reveal movements in the  $\beta 1$  and  $\beta 2$  strands. Molecular dynamic (MD) simulations of *C. elegans* GluCl deactivation show that the loop connecting  $\beta 1$  and  $\beta 2$  strands moves towards the TM2-3 loop (Calimet *et al.*, 2013). This movement appears to precede conformational changes within the TM domains which lead to gating. Furthermore, mutations that prevent the electrostatic interaction between the  $\beta 1$ - $\beta 2$  loop and the TM2-3 loop in the GABA<sub>A</sub>  $\alpha 1$  subunit reduce GABA efficacy (Kash *et al.*, 2003). We have also previously demonstrated that substitution of the conserved  $\alpha 1$  subunit TM2-3 Lys278 by methionine reduces the efficacy of GABA (Hales *et al.*, 2006). These functional, structural and simulation data, together with our current findings, suggest that the movement of loop G residues is involved in a series of structural rearrangements required for normal channel gating.

GABA-evoked currents mediated by  $\alpha 1(D43C)\beta 2\gamma 2$  and  $\alpha 1(T47R)\beta 2\gamma 2$  receptors exhibit a dramatically increased deactivation rate compared to WT receptors. There were also changes to apparent desensitisation kinetics and a tendency towards slowed activation rate.  $\alpha 1(F64C)$  and  $\alpha 1(F64T)$  substitutions in loop D caused more substantial changes in macroscopic current kinetics, with activation, apparent desensitisation and deactivation rates all significantly affected. This is consistent with the dual binding and gating role played by Phe64 in loop D (Boileau *et al.*, 1999; Szcot *et al.*, 2014). These changes in kinetics, particularly the observed increase in deactivation rates, are consistent with those we have previously observed for the  $\alpha 1(K278M)$  substitution, at the TM2-3 loop location, far removed from the agonist binding site, which also impairs agonist efficacy (Hales *et al.*, 2006; Othman *et al.*, 2012). In this case faster deactivation reflected a reduced mean open time. Reduced mean open time may also account for the increase in deactivation rates for  $\alpha 1(D43C)\beta 2\gamma 2$  and  $\alpha 1(T47R)\beta 2\gamma 2$  receptors as both substitutions caused reduced  $P_{open}$  compared to WT receptors.

Ligand binding experiments indicate that GABA cannot dissociate from homomeric  $\rho 1$  receptors in the open channel conformation (Chang & Weiss, 1999). Similarly GABA becomes trapped in its binding sites on  $\alpha 1\beta 3\gamma 2$  receptors and does not unbind until the channel closes (Bianchi & Macdonald, 2001). Therefore the deactivation time course is largely dictated by the mean open time of the receptor. Our data demonstrate that THIP-evoked currents deactivate faster than GABA-evoked currents, consistent with single channel data demonstrating a shorter mean open time associated with activation by the partial agonist (Mortensen *et al.*, 2004).

Our data indicate that the efficacy of THIP is severely impaired in the presence of the  $\alpha 1(T47R)$  substitution. It is worth noting that the macroscopic current kinetics of THIP-evoked currents in  $\alpha 1(T47R)\beta 2\gamma 2$  receptors begin to resemble those with the loop D  $\alpha 1(F64C)$  and  $\alpha 1(F64T)$  substitutions. This may suggest that as agonist efficacy becomes progressively impaired, there may be incremental changes to activation, apparent desensitisation and deactivation rates.

We have previously observed that reduced efficacy associated with the  $\alpha 1(K278M)$  substitution, was not restricted to GABA but also generalised to activation by propofol (Hales *et al.*, 2006). Consistent with a similar scenario, propofol-evoked currents mediated by  $\alpha 1(T47R)\beta 2\gamma 2$  receptors also deactivate faster than their WT counterparts, suggesting that the mean open times for propofol-activated channels were also reduced by the  $\alpha 1(T47R)$  substitution. These data confirm that the  $\alpha 1(T47R)$  substitution impairs gating through a mechanism independent of orthosteric binding and suggest a common conformational rearrangement associated with activation by orthosteric and allosteric agonists.

We also examined the effect of  $\alpha 1(T47R)$  substitution on spontaneous gating to further explore the generality of its ability to impair gating. Our previous work demonstrates that WT  $GABA_A$  receptors exhibit a low level of spontaneous gating that can be blocked by the non-competitive inhibitor picrotoxin and the inverse agonist bicuculline (McCartney *et al.*, 2007). The  $\alpha 1(K278M)$  substitution, which inhibits GABA and propofol efficacy also reduces spontaneous gating (Othman *et al.*, 2012).

In order to examine the effects of the loop G and loop D substitutions on gating that is independent of any agonist, we used the L285R substitution in the  $\beta 2$  subunit to enhance spontaneous gating. A previous study of  $\beta 1(L285R)$  demonstrated that the substitution caused a large increase in GABA-independent gating (Anstee *et al.*, 2013). Consistent with this,  $\alpha 1\beta 2(L285R)\gamma 2$  receptors also exhibited marked spontaneous currents that were inhibited by picrotoxin. Spontaneous gating was reduced in  $\alpha 1(T47R)\beta 2(L285R)\gamma 2$  compared to  $\alpha 1\beta 2(L285R)\gamma 2$  receptors confirming that, like  $\alpha 1(K278M)$ ,  $\alpha 1(T47R)$  impairs gating independently of agonist activation.

In summary this study suggests that movement of loop G in the  $\beta 1$  strand of the  $GABA_A$  receptor  $\alpha 1$  subunit is involved in a conformational rearrangement associated with channel activation. The non-conservative replacements of Asp43 and Thr47 reduce efficacy presumably by impeding movement of the entire  $\beta 1$ - $\beta 2$  antiparallel loop structure. The importance of this region of pLGICs in activation by orthosteric agonists might have been predicted by structural data and MD simulations (Calimet *et al.*, 2013; Althoff *et al.*, 2014; Du *et al.*, 2015).

Kinetic models of glycine and nicotinic acetylcholine receptor gating incorporate pre-open shut states, termed flip and prime, respectively (Burzomato *et al.*, 2004; Mukhtasimova *et al.*, 2009). The rates of transition into these states correlate with agonist efficacy (Lape *et al.*, 2008). It is therefore not a surprise that the  $\alpha 1$ (F64C) substitution in loop D, which reduces the efficacy of GABA, also reduces the transition rate constants into the flip state (Szczot *et al.*, 2014). It is possible that the D43C and T47R substitutions also hinder these pre-open transitions. Perhaps more surprisingly, however, the T47R substitution also impairs gating that is independent of orthosteric (or indeed allosteric) agonist activation.

A requirement for the movement of loop G residues during agonist independent gating may provide a mechanism for the negative efficacy that is characteristic of inverse agonism. It is possible that bicuculline inhibits GABA<sub>A</sub> receptor gating, caused by either allosteric or spontaneous activation, by immobilising the antiparallel  $\beta 1$ - $\beta 2$  strand structure (McCartney *et al.*, 2007). Additional structural studies will be required to test this hypothesis.

## References

- Althoff T, Hibbs RE, Banerjee S & Gouaux E. (2014). X-ray structures of GluCl in apo states reveal a gating mechanism of Cys-loop receptors. *Nature* **512**, 333-337.
- Anstee QM, Knapp S, Maguire EP, Hosie AM, Thomas P, Mortensen M, Bhome R, Martinez A, Walker SE, Dixon CI, Ruparella K, Montagnese S, Kuo YT, Herlihy A, Bell JD, Robinson I, Guerrini I, McQuillin A, Fisher EM, Ungless MA, Gurling HM, Morgan MY, Brown SD, Stephens DN, Belelli D, Lambert JJ, Smart TG & Thomas HC. (2013). Mutations in the Gabrb1 gene promote alcohol consumption through increased tonic inhibition. *Nat Commun* **4**, 2816.
- Baptista-Hon DT, Deeb TZ, Lambert JJ, Peters JA & Hales TG. (2013). The minimum M3-M4 loop length of neurotransmitter-activated pentameric receptors is critical for the structural integrity of cytoplasmic portals. *J Biol Chem* **288**, 21558-21568.
- Baptista-Hon DT, Krah A, Zachariae U & Hales TG. (2016). A role for loop G in the beta1 strand in GABA receptor activation. *J Physiol*.
- Berger O, Edholm O & Jahnig F. (1997). Molecular dynamics simulations of a fluid bilayer of dipalmitoylphosphatidylcholine at full hydration, constant pressure, and constant temperature. *Biophys J* **72**, 2002-2013.
- Bianchi MT & Macdonald RL. (2001). Agonist Trapping by GABAA Receptor Channels. *J Neurosci* **21**, 9083-9091.
- Boileau AJ, Evers AR, Davis AF & Czajkowski C. (1999). Mapping the agonist binding site of the GABAA receptor: evidence for a beta-strand. *J Neurosci* **19**, 4847-4854.
- Boileau AJ, Newell JG & Czajkowski C. (2002). GABA(A) receptor beta 2 Tyr97 and Leu99 line the GABA-binding site. Insights into mechanisms of agonist and antagonist actions. *J Biol Chem* **277**, 2931-2937.
- Burzomato V, Beato M, Groot-Kormelink PJ, Colquhoun D & Sivilotti LG. (2004). Single-channel behavior of heteromeric alpha1beta glycine receptors: an attempt to detect a conformational change before the channel opens. *J Neurosci* **24**, 10924-10940.
- Calimet N, Simoes M, Changeux JP, Karplus M, Taly A & Cecchini M. (2013). A gating mechanism of pentameric ligand-gated ion channels. *Proc Natl Acad Sci U S A* **110**, E3987-3996.

This is an Accepted Article that has been peer-reviewed and approved for publication in the The Journal of Physiology, but has yet to undergo copy-editing and proof correction. Please cite this article as an 'Accepted Article'; [doi: 10.1113/JP273752](https://doi.org/10.1113/JP273752).

This article is protected by copyright. All rights reserved.



- Colquhoun D. (1998). Binding, gating, affinity and efficacy: the interpretation of structure-activity relationships for agonists and of the effects of mutating receptors. *Br J Pharmacol* **125**, 924-947.
- Cromer BA, Morton CJ & Parker MW. (2002). Anxiety over GABA(A) receptor structure relieved by AChBP. *Trends in biochemical sciences* **27**, 280-287.
- Du J, Lu W, Wu S, Cheng Y & Gouaux E. (2015). Glycine receptor mechanism elucidated by electron cryo-microscopy. *Nature*.
- Goldschen-Ohm MP, Wagner DA & Jones MV. (2011). Three arginines in the GABAA receptor binding pocket have distinct roles in the formation and stability of agonist- versus antagonist-bound complexes. *Molecular pharmacology* **80**, 647-656.
- Hadley SH & Amin J. (2007). Rat alpha6beta2delta GABAA receptors exhibit two distinct and separable agonist affinities. *J Physiol* **581**, 1001-1018.
- Hales TG, Deeb TZ, Tang H, Bollan KA, King DP, Johnson SJ & Connolly CN. (2006). An asymmetric contribution to gamma-aminobutyric type A receptor function of a conserved lysine within TM2-3 of alpha1, beta2, and gamma2 subunits. *J Biol Chem* **281**, 17034-17043.
- Heckman KL & Pease LR. (2007). Gene splicing and mutagenesis by PCR-driven overlap extension. *Nat Protoc* **2**, 924-932.
- Hibbs RE & Gouaux E. (2011). Principles of activation and permeation in an anion-selective Cys-loop receptor. *Nature* **474**, 54-60.
- Hinkle DJ & Macdonald RL. (2003). Beta subunit phosphorylation selectively increases fast desensitization and prolongs deactivation of alpha1beta1gamma2L and alpha1beta3gamma2L GABA(A) receptor currents. *J Neurosci* **23**, 11698-11710.
- Holden JH & Czajkowski C. (2002). Different residues in the GABA(A) receptor alpha 1T60-alpha 1K70 region mediate GABA and SR-95531 actions. *J Biol Chem* **277**, 18785-18792.
- Kash TL, Jenkins A, Kelley JC, Trudell JR & Harrison NL. (2003). Coupling of agonist binding to channel gating in the GABA(A) receptor. *Nature* **421**, 272-275.
- Lape R, Colquhoun D & Sivilotti LG. (2008). On the nature of partial agonism in the nicotinic receptor superfamily. *Nature* **454**, 722-727.

- McCartney MR, Deeb TZ, Henderson TN & Hales TG. (2007). Tonicly active GABAA receptors in hippocampal pyramidal neurons exhibit constitutive GABA-independent gating. *Molecular pharmacology* **71**, 539-548.
- Miller PS & Aricescu AR. (2014). Crystal structure of a human GABA receptor. *Nature*.
- Morales-Perez CL, Noviello CM & Hibbs RE. (2016). X-ray structure of the human alpha4beta2 nicotinic receptor. *Nature* **538**, 411-415.
- Mortensen M, Kristiansen U, Ebert B, Frolund B, Krogsgaard-Larsen P & Smart TG. (2004). Activation of single heteromeric GABA(A) receptor ion channels by full and partial agonists. *J Physiol* **557**, 389-413.
- Mukhtasimova N, Lee WY, Wang HL & Sine SM. (2009). Detection and trapping of intermediate states priming nicotinic receptor channel opening. *Nature* **459**, 451-454.
- Newell JG & Czajkowski C. (2003). The GABAA receptor alpha 1 subunit Pro174-Asp191 segment is involved in GABA binding and channel gating. *J Biol Chem* **278**, 13166-13172.
- Othman NA, Gallacher M, Deeb TZ, Baptista-Hon DT, Perry DC & Hales TG. (2012). Influences on blockade by t-butylbicyclo-phosphoro-thionate of GABA(A) receptor spontaneous gating, agonist activation and desensitization. *J Physiol* **590**, 163-178.
- Smith GB & Olsen RW. (1995). Functional domains of GABAA receptors. *Trends in pharmacological sciences* **16**, 162-168.
- Szczot M, Kisiel M, Czyzewska MM & Mozrzykmas JW. (2014). alpha1F64 Residue at GABA(A) receptor binding site is involved in gating by influencing the receptor flipping transitions. *J Neurosci* **34**, 3193-3209.
- Tran PN, Laha KT & Wagner DA. (2011). A tight coupling between beta(2)Y97 and beta(2)F200 of the GABA(A) receptor mediates GABA binding. *J Neurochem* **119**, 283-293.
- Venkatachalan SP & Czajkowski C. (2008). A conserved salt bridge critical for GABA(A) receptor function and loop C dynamics. *Proc Natl Acad Sci U S A* **105**, 13604-13609.
- Wagner DA, Czajkowski C & Jones MV. (2004). An arginine involved in GABA binding and unbinding but not gating of the GABA(A) receptor. *J Neurosci* **24**, 2733-2741.
- Whiting PJ, McKernan RM & Wafford KA. (1995). Structure and pharmacology of vertebrate GABAA receptor subtypes. *International review of neurobiology* **38**, 95-138.

**Additional Information**

Competing interests – The authors declare no competing financial interests.

Author contributions – D.T.B-H and T.G.H. designed the study. D.T.B-H and S.G. acquired the data. D.T.B-H, S.G. and T.G.H. analysed and interpreted the data. D.T.B-H and T.G.H drafted the work and revised it critically for intellectual content. All authors approved the final version of this manuscript and agree to be accountable for all aspects of the work in ensuring that questions relating to the accuracy and integrity of the work are appropriately investigated and resolved. All authors qualify for authorship and only those who qualify for authorship are listed.

Funding – This work was supported by funding from Tenovus Scotland.

## Figure legends

**Figure 1.** Loop G and loop D of *C. elegans* GluCl and GABA<sub>A</sub> receptor  $\alpha$  subunits. **A**, Amino acid sequence alignment of the mouse GABA<sub>A</sub>  $\alpha$ 1 to  $\alpha$ 6 subunits and GluCl  $\alpha$  subunit. The  $\beta$ 1 and  $\beta$ 2 strands are highlighted in green and red, respectively. Residues in loop G and D of the GABA<sub>A</sub>  $\alpha$ 1 subunit are underlined. Also underlined are the homologous residues on the GABA<sub>A</sub>  $\alpha$ 2 to  $\alpha$ 6 and GluCl which are relevant to this study. **B**, The *C. elegans* GluCl (Hibbs & Gouaux, 2011) model, showing the interface between two subunits (blue – primary interface, yellow – complimentary interface) with the  $\beta$ 1 and  $\beta$ 2 strands highlighted (green and red, respectively). Bound glutamate is shown in grey. Inset shows the highlighted area in more detail. Asn33 and Arg37 are shown on the  $\beta$ 1 strand as stick rendering in green. Thr54 is shown on the  $\beta$ 2 strand as stick rendering in red. **C**, Representative examples of whole-cell currents evoked by a maximal and an approximate EC<sub>50</sub> concentration of GABA (indicated) mediated by  $\alpha$ 1 $\beta$ 2 $\gamma$ 2 or  $\alpha$ 1(T47R) $\beta$ 2 $\gamma$ 2 GABA<sub>A</sub> receptors. The bar indicates GABA application (2 s). **D**, Concentration-response relationships for  $\alpha$ 1 $\beta$ 2 $\gamma$ 2 (circles) or  $\alpha$ 1(T47R) $\beta$ 2 $\gamma$ 2 (triangles) receptors. Current amplitudes were expressed as a percentage of the maximum current amplitude recorded from each cell. The sigmoidal curve represents the logistic function fitted to the data points.

**Figure 2.** The identity of Loop G and loop D residues influences agonist efficacy. **A**, Representative examples of whole-cell currents mediated by  $\alpha$ 1 $\beta$ 2 $\gamma$ 2,  $\alpha$ 1(D43C) $\beta$ 2 $\gamma$ 2  $\alpha$ 1(T47R) $\beta$ 2 $\gamma$ 2 or  $\alpha$ 1(F64C) $\beta$ 2 $\gamma$ 2 receptors evoked by a maximal concentration of GABA alone (black traces) or in the presence of 1  $\mu$ M propofol (grey traces). The concentration of GABA used was 1 mM for  $\alpha$ 1 $\beta$ 2 $\gamma$ 2, 300 mM for  $\alpha$ 1(D43C) $\beta$ 2 $\gamma$ 2 and 30 mM for  $\alpha$ 1(T47R) $\beta$ 2 $\gamma$ 2 and 300 mM for  $\alpha$ 1(F64C) $\beta$ 2 $\gamma$ 2 receptors. Propofol potentiated GABA-evoked currents mediated by  $\alpha$ 1(D43C) $\beta$ 2 $\gamma$ 2,  $\alpha$ 1(T47R) $\beta$ 2 $\gamma$ 2 and  $\alpha$ 1(F64C) $\beta$ 2 $\gamma$ 2 receptors. **B**, Bar graph shows mean percentage potentiation by propofol. Propofol significantly potentiated GABA-evoked currents mediated by  $\alpha$ 1(D43C) $\beta$ 2 $\gamma$ 2,  $\alpha$ 1(T47R) $\beta$ 2 $\gamma$ 2 and  $\alpha$ 1(F64C) $\beta$ 2 $\gamma$ 2 receptors (\*  $P < 0.05$ ,  $P < 0.001$  and  $P < 0.0001$ , respectively; one-way ANOVA *post-hoc* Tukey's comparison). There was also a statistically significant difference between  $\alpha$ 1(F64C) $\beta$ 2 $\gamma$ 2 receptors and  $\alpha$ 1(D43C) $\beta$ 2 $\gamma$ 2 or  $\alpha$ 1(T47R) $\beta$ 2 $\gamma$ 2 receptors (#  $P < 0.05$  and  $P < 0.001$ , respectively; one-way ANOVA *post-hoc* Tukey's comparison).

**Figure 3.** Maximal  $P_{open}$  is reduced in  $\alpha 1(D43C)\beta 2\gamma 2$  and  $\alpha 1(T47R)\beta 2\gamma 2$  receptors. **A**, Representative examples of variance and mean current calculated from 10 consecutive GABA applications to  $\alpha 1\beta 2\gamma 2$  or  $\alpha 1(T47R)\beta 2\gamma 2$  receptors. The application of GABA is indicated by the liquid junction current above each trace. Only the variance and mean current values following the peak of the current (black) were used in the analysis. **B**, Mean current versus variance plot for  $\alpha 1\beta 2\gamma 2$  or  $\alpha 1(T47R)\beta 2\gamma 2$  receptors. The dotted line represents the parabolic function fitted to the data points. **C**, Bar graph of mean single channel conductances. The single channel conductance for  $\alpha 1\beta 2\gamma 2$ ,  $\alpha 1(D43C)\beta 2\gamma 2$  and  $\alpha 1(T47R)\beta 2\gamma 2$  receptors were  $26 \pm 3.2$  pS ( $n = 8$ ),  $27 \pm 2.9$  pS ( $n = 7$ ) and  $26 \pm 2.3$  pS ( $n = 5$ ) respectively. There was no significant difference between the means ( $P = 0.96$ ; one-way ANOVA). **D**, Bar graph of mean maximal  $P_{open}$  for  $\alpha 1\beta 2\gamma 2$ ,  $\alpha 1(D43C)\beta 2\gamma 2$  and  $\alpha 1(T47R)\beta 2\gamma 2$  receptors. There was a statistically significant difference in  $P_{open}$  between  $\alpha 1\beta 2\gamma 2$  and  $\alpha 1(D43C)\beta 2\gamma 2$  receptors and between WT  $\alpha 1\beta 2\gamma 2$  and  $\alpha 1(T47R)\beta 2\gamma 2$  receptors (\*  $P < 0.05$ ; one-way ANOVA; *post-hoc* Tukey's comparison).

**Figure 4.** The kinetics of GABA-evoked currents mediated by  $\alpha 1\beta 2\gamma 2$ ,  $\alpha 1(D43C)\beta 2\gamma 2$ ,  $\alpha 1(T47R)\beta 2\gamma 2$ ,  $\alpha 1(F64C)\beta 2\gamma 2$  and  $\alpha 1(F64T)\beta 2\gamma 2$  receptors. **A**, Representative examples of GABA-evoked currents mediated by  $\alpha 1\beta 2\gamma 2$ ,  $\alpha 1(D43C)\beta 2\gamma 2$ ,  $\alpha 1(T47R)\beta 2\gamma 2$  and  $\alpha 1(F64C)\beta 2\gamma 2$  receptors recorded from outside-out patches. The associated square pulses indicate the junction currents corresponding to agonist application. **B**, (inset) Representative examples of amplitude-normalised activation phases of GABA-evoked currents mediated by  $\alpha 1\beta 2\gamma 2$  (black),  $\alpha 1(T47R)\beta 2\gamma 2$  (grey) or  $\alpha 1(F64C)\beta 2\gamma 2$  (grey) receptors. Bar graph shows mean 10-90% rise time of current activation. Both  $\alpha 1(F64C)$  and  $\alpha 1(F64T)$  substitutions significantly slowed the GABA-activation rate when compared with  $\alpha 1\beta 2\gamma 2$  receptors (\*  $P < 0.0001$ ; one-way ANOVA *post-hoc* Tukey's comparison) and with  $\alpha 1(D43C)\beta 2\gamma 2$  or  $\alpha 1(T47R)\beta 2\gamma 2$  receptors (#  $P < 0.0001$ ; one-way ANOVA *post-hoc* Tukey's comparison). **C**, Bar graph shows the mean percentage current remaining. GABA-evoked currents mediated by  $\alpha 1(D43C)\beta 2\gamma 2$ ,  $\alpha 1(F64C)\beta 2\gamma 2$  and  $\alpha 1(F64T)\beta 2\gamma 2$  receptors desensitise significantly less, when compared with  $\alpha 1\beta 2\gamma 2$  receptors ( $P < 0.05$ ;  $P < 0.001$  and  $P < 0.001$ , respectively; one-way ANOVA *post-hoc* Tukey's comparison). **D**, Mean desensitisation  $\tau_w$  of  $\alpha 1\beta 2\gamma 2$ ,  $\alpha 1(D43C)\beta 2\gamma 2$  and  $\alpha 1(T47R)\beta 2\gamma 2$  receptors. There was no statistically significant difference in mean  $\tau_w$  ( $P = 0.08$ ; one-way ANOVA). The individual components of the multi-exponential fit is summarised in Table 1. **E**, (inset) Representative examples of amplitude-normalised current deactivation following agonist removal. The superimposed traces are time-shifted for clarity. The step above each trace indicates the liquid junction current corresponding to agonist removal. The bar graph shows mean deactivation  $\tau_w$ . GABA-evoked currents mediated by  $\alpha 1(D43C)\beta 2\gamma 2$ ,  $\alpha 1(T47R)\beta 2\gamma 2$ ,  $\alpha 1(F64C)\beta 2\gamma 2$  and  $\alpha 1(F64T)\beta 2\gamma 2$  receptors

deactivated significantly faster when compared to those mediated by  $\alpha 1\beta 2\gamma 2$  receptors (\*  $P < 0.0001$ ; one-way ANOVA *post-hoc* Tukey's comparison). The individual components of the multi-exponential fits are summarised in Table 2.

**Figure 5.** The kinetics of GABA- and THIP-evoked currents mediated by  $\alpha 1\beta 2\gamma 2$  or  $\alpha 1(T47R)\beta 2\gamma 2$  receptors. **A**, Representative examples of maximal GABA- (black) and THIP-evoked (grey) currents recorded from excised outside-out patches containing  $\alpha 1\beta 2\gamma 2$  or  $\alpha 1(T47R)\beta 2\gamma 2$  receptors. The upward (black) and downward (grey) steps above each correspond to the liquid junction current for GABA and THIP application, respectively. **B**, The mean maximum THIP-evoked current amplitude (as percentage of maximal GABA current amplitude) was significantly less than the maximum GABA-evoked current amplitude at  $\alpha 1\beta 2\gamma 2$  receptors (#  $P = 0.002$ ; paired t-test). The efficacy of THIP was significantly reduced at  $\alpha 1(T47R)\beta 2\gamma 2$  receptors (\*  $P = 0.0001$ ; t-test). **C**, Representative examples of the activation phases of GABA- (black) and THIP-evoked (grey) currents recorded from excised outside-out patches containing  $\alpha 1\beta 2\gamma 2$  receptors. The associated graph illustrates the mean 10-90% rise times. THIP-evoked currents activated significantly slower than GABA-evoked currents (\*  $P = 0.0001$ ; t-test). **D**, Bar graph shows mean desensitisation  $\tau_w$ . THIP-evoked currents desensitised significantly more slowly than GABA-evoked currents (\*  $P = 0.0011$ ; t-test). **E**, Representative examples show amplitude-normalised deactivation phases of GABA- (black) and THIP-evoked (grey) currents. Bar graph shows mean deactivation  $\tau_w$ . THIP-evoked currents deactivated significantly faster than GABA-evoked currents (\*  $P = 0.0001$ ; t-test). **F**, Representative activation phases of THIP-evoked currents from outside-out patches containing  $\alpha 1\beta 2\gamma 2$  (black) and  $\alpha 1(T47R)\beta 2\gamma 2$  (grey) receptors. Bar graph shows mean 10-90% rise times. The  $\alpha 1(T47R)$  substitution significantly slowed the activation rates of THIP-evoked currents, as compared to WT receptors (\*  $P = 0.002$ ; t-test). **G**, Bar graph shows mean percentage current remaining. THIP-evoked currents show less desensitisation as compared to  $\alpha 1\beta 2\gamma 2$  receptors (\*  $P = 0.0001$ ; t-test). **H**, Representative examples of amplitude-normalised deactivation phases of THIP-evoked currents mediated by  $\alpha 1\beta 2\gamma 2$  (black) and  $\alpha 1(T47R)\beta 2\gamma 2$  (grey) receptors. Bar graph shows mean deactivation  $\tau_w$ . The  $\alpha 1(T47R)$  substitution significantly increased deactivation rate (\*  $P = 0.0001$ ; t-test).

**Figure 6.** The kinetics of propofol-evoked currents mediated by  $\alpha 1\beta 2\gamma 2$ ,  $\alpha 1(T47R)\beta 2\gamma 2$  and  $\alpha 1(F64C)\beta 2\gamma 2$  receptors. **A**, Representative examples of propofol-evoked currents mediated by  $\alpha 1\beta 2\gamma 2$ ,  $\alpha 1(T47R)\beta 2\gamma 2$  and  $\alpha 1(F64C)\beta 2\gamma 2$  receptors recorded from excised outside-out patches. The square pulse above each trace indicates the time-course of solution exchange. **B**, Representative examples of amplitude-normalised activation phases of propofol-evoked currents mediated by  $\alpha 1\beta 2\gamma 2$  (black),  $\alpha 1(T47R)\beta 2\gamma 2$  (grey) and  $\alpha 1(F64C)\beta 2\gamma 2$  (grey) receptors. The bar graph shows the

mean 10-90% rise time of current activation. There were no statistically significant differences in the activation rates of propofol-evoked currents. **C**, Representative examples of amplitude-normalised decaying phases of the currents depicted in **A**, following propofol removal. The superimposed traces are time-shifted for clarity. The step above each trace indicates the liquid junction current corresponding to agonist removal. The bar graph shows mean deactivation  $\tau_w$ . Propofol-evoked currents mediated by  $\alpha 1(T47R)\beta 2\gamma 2$  and  $\alpha 1(F64C)\beta 2\gamma 2$  receptors deactivated significantly faster when compared to those mediated by  $\alpha 1\beta 2\gamma 2$  receptors (\*  $P < 0.0001$  for both; one-way ANOVA *post-hoc* Tukey's comparison). Mean kinetic parameters are summarised in Table 1.

**Figure 7.** Spontaneous gating mediated by  $\alpha 1\beta 2\gamma 2$ ,  $\alpha 1\beta 2(L285R)\gamma 2$  and  $\alpha 1(T47R)\beta 2(L285R)\gamma 2$  receptors. **A**, Representative examples of GABA-evoked currents (black traces) and inhibition of spontaneous currents by picrotoxin (grey traces) mediated by  $\alpha 1\beta 2\gamma 2$ ,  $\alpha 1\beta 2(L285R)\gamma 2$  and  $\alpha 1(T47R)\beta 2(L285R)\gamma 2$  receptors. **B**, Bar graph shows mean percentage spontaneous current (expressed as  $I_{\text{spont}}/I_{\text{GABA}}$ ). One-way ANOVA revealed a statistically significant difference in mean spontaneous current ( $P < 0.0001$ ). Mean spontaneous current amplitudes differed between  $\alpha 1\beta 2\gamma 2$  and  $\alpha 1\beta 2(L285R)\gamma 2$  receptors (\*  $P < 0.0001$ ) and between  $\alpha 1\beta 2(L285R)\gamma 2$  and  $\alpha 1(T47R)\beta 2(L285R)\gamma 2$  receptors (#  $P < 0.0001$ ; *post-hoc* Tukey's comparison).

Table 1. Summary of desensitisation components.

	Agonist	$\tau_f$	% <sub>f</sub>	$\tau_m$	% <sub>m</sub>	$\tau_s$	% <sub>s</sub>	$\tau_w$
$\alpha 1\beta 2\gamma 2$	GABA	3.2 ± 0.34	27 ± 3.0	36 ± 6.3	30 ± 6.0	410 ± 49	43 ± 4.5	190 ± 25
	THIP	4.6	7.5 ± 5.8 #	33 ± 5.9	31 ± 5.0	350 ± 34	61 ± 6.5 #	240 ± 35
$\alpha 1(D43C)\beta 2\gamma 2$	GABA	6.7 ± 1.9 *	21 ± 6.1	42 ± 7.0	11 ± 4.3	460 ± 110	68 ± 7.0 *	320 ± 87
$\alpha 1(T47R)\beta 2\gamma 2$	GABA	4.6 ± 0.94	13 ± 3.7 *	50 ± 7.7	18 ± 3.7	790 ± 220	69 ± 4.6 *	570 ± 170

# P < 0.05 (unpaired t-test) compared with the equivalent WT GABA-evoked current value.

\* P < 0.05 (one-way ANOVA *post-hoc* Tukey's comparison) compared with GABA-evoked currents mediated by  $\alpha 1\beta 2\gamma 2$  receptors.

This is an Accepted Article that has been peer-reviewed and approved for publication in the The Journal of Physiology, but has yet to undergo copy-editing and proof correction. Please cite this article as an 'Accepted Article'; [doi: 10.1113/JP273752](https://doi.org/10.1113/JP273752).

This article is protected by copyright. All rights reserved.



Table 2. Summary of deactivation components.

	Agonist	$\tau_f$	% <sub>f</sub>	$\tau_m$	% <sub>m</sub>	$\tau_s$	% <sub>s</sub>	$\tau_w$
$\alpha 1\beta 2\gamma 2$	GABA	11 ± 2.0	8.1 ± 3.7	47 ± 5.6	61 ± 5.2	270 ± 54	30 ± 5.0	100 ± 17
	THIP	3.2 ± 0.89 #	40 ± 8.4 #	12 ± 1.7 #	61 ± 7.1	68 ± 13 #	6.1 ± 1.5 #	12 ± 1.4 #
$\alpha 1(D43C)\beta 2\gamma 2$	GABA	7.9 ± 1.8	64 ± 3.1 *	45 ± 12	28 ± 2.6 *	280 ± 110	7.5 ± 2.6 *	34 ± 8.7 *
$\alpha 1(T47R)\beta 2\gamma 2$	GABA	0.91 ± 0.094 *	73 ± 5.4 *	8.4 ± 2.2	25 ± 5.3 *	140 ± 27	2.3 ± 0.32 *	4.4 ± 0.47 *
	THIP	0.93 ± 0.076	93 ± 1.6 #	20 ± 4.5 #	7.0 ± 1.6 #	NA	NA	2.2 ± 0.46 #
$\alpha 1(F64C)\beta 2\gamma 2$	GABA	1.9 ± 0.62 *	91 ± 5.4 *	42 ± 15	8.5 ± 5.4 *	NA	NA	3.5 ± 1.3 *
$\alpha 1(F64T)\beta 2\gamma 2$	GABA	0.83 ± 0.071 *	93 ± 1.5 *	72 ± 24	6.6 ± 1.5 *	NA	NA	6.2 ± 2.5 *

# P < 0.05 (unpaired t-test) compared with the equivalent GABA-evoked current value.

\* P < 0.05 (one-way ANOVA *post-hoc* Tukey's comparison) compared with GABA-evoked currents mediated by  $\alpha 1\beta 2\gamma 2$  receptors.

NA – not applicable due to a loss of this component.

Fig. 1

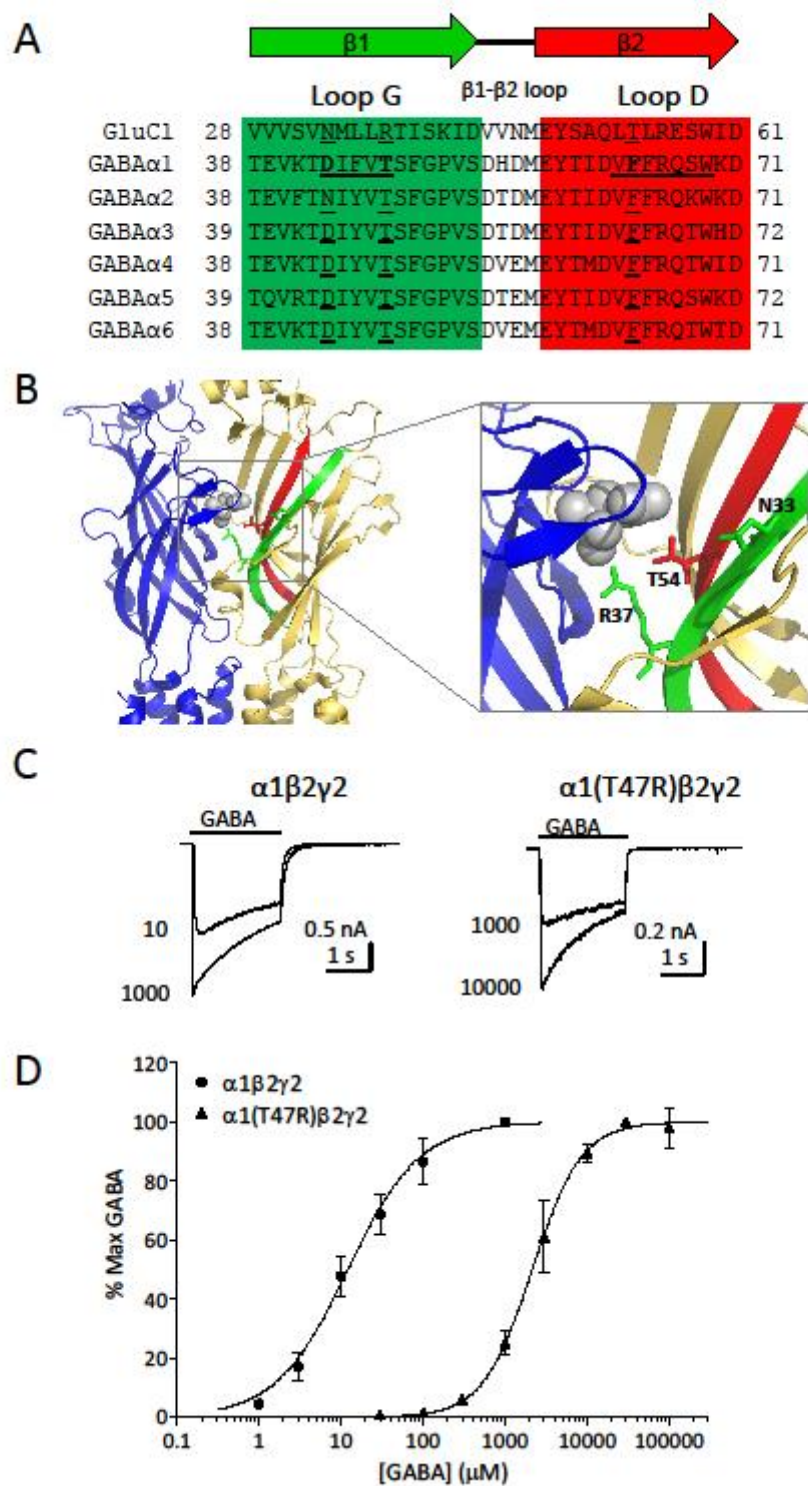


Fig. 2

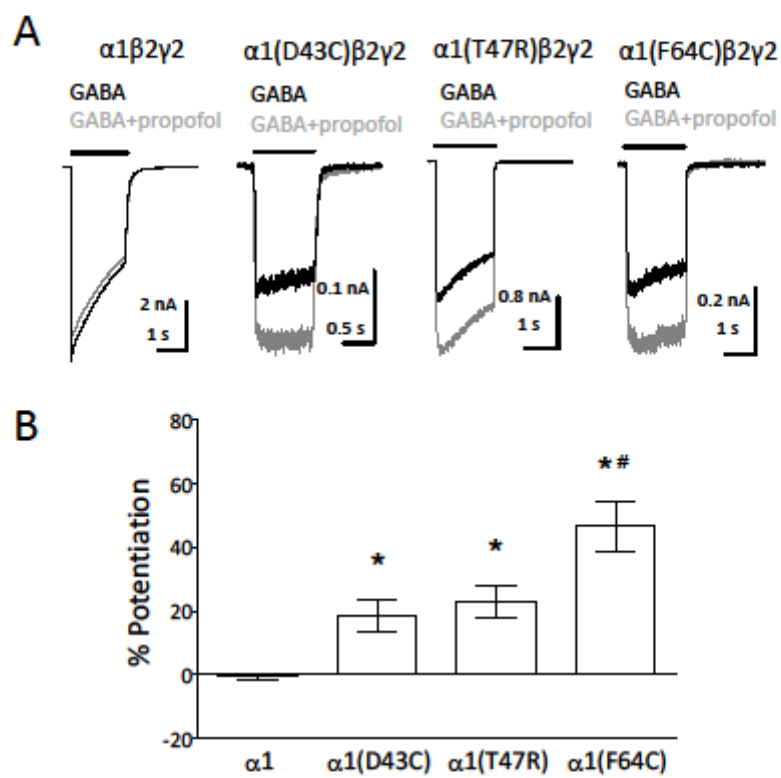


Fig. 3

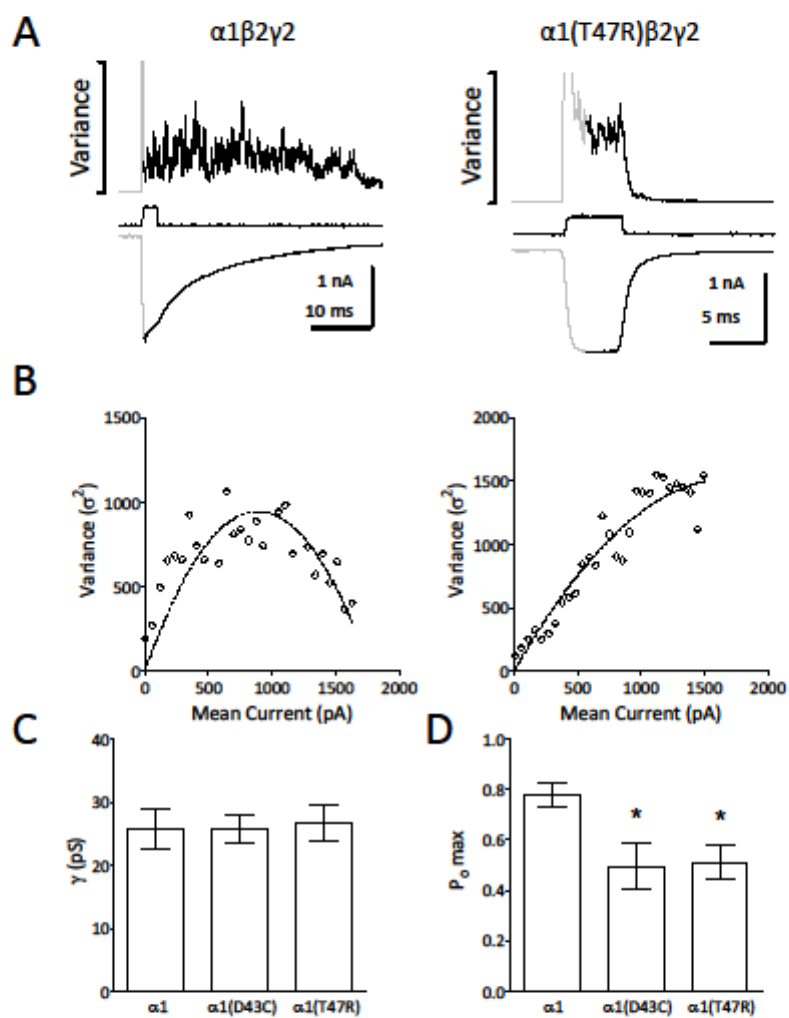


Fig. 4

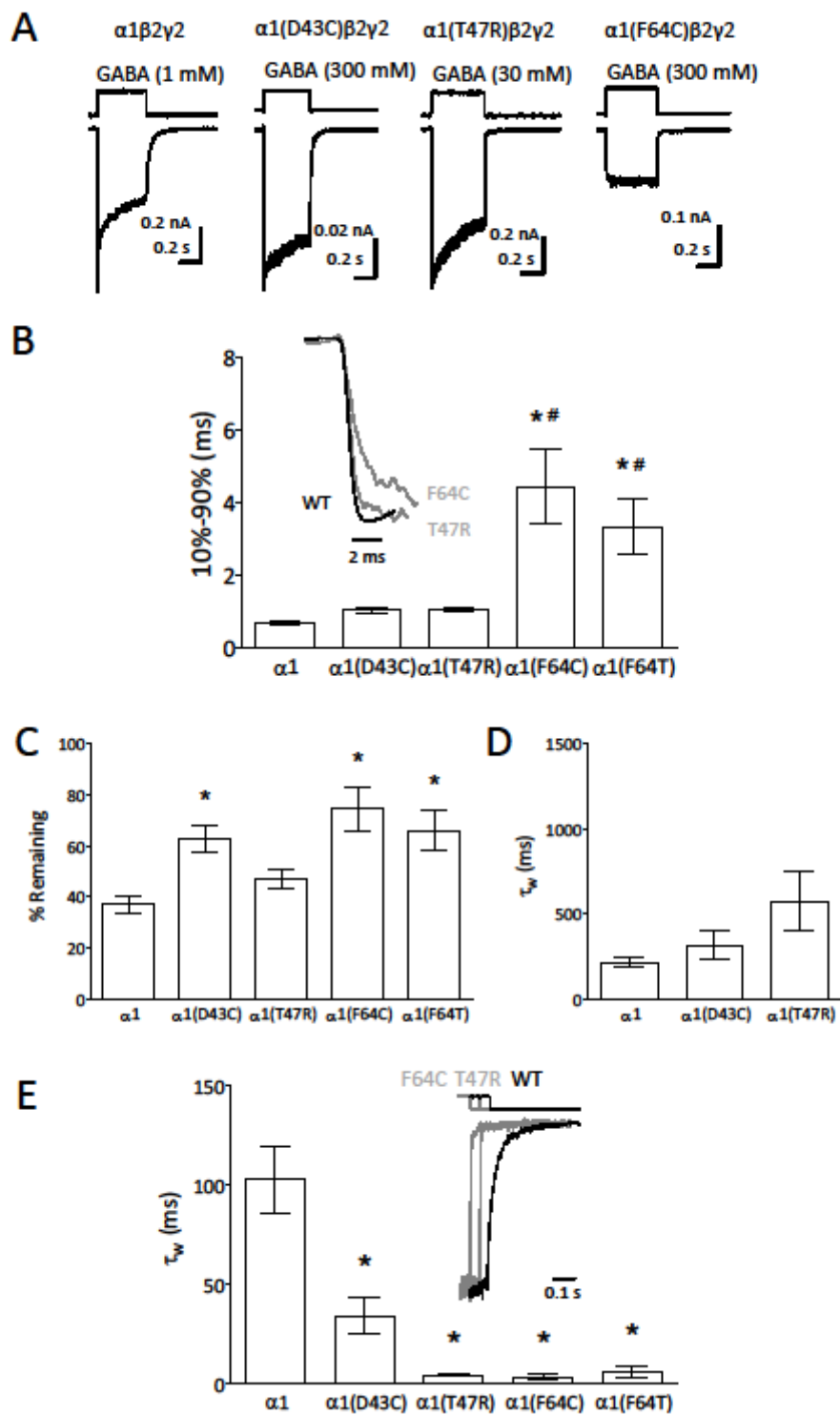


Fig. 5

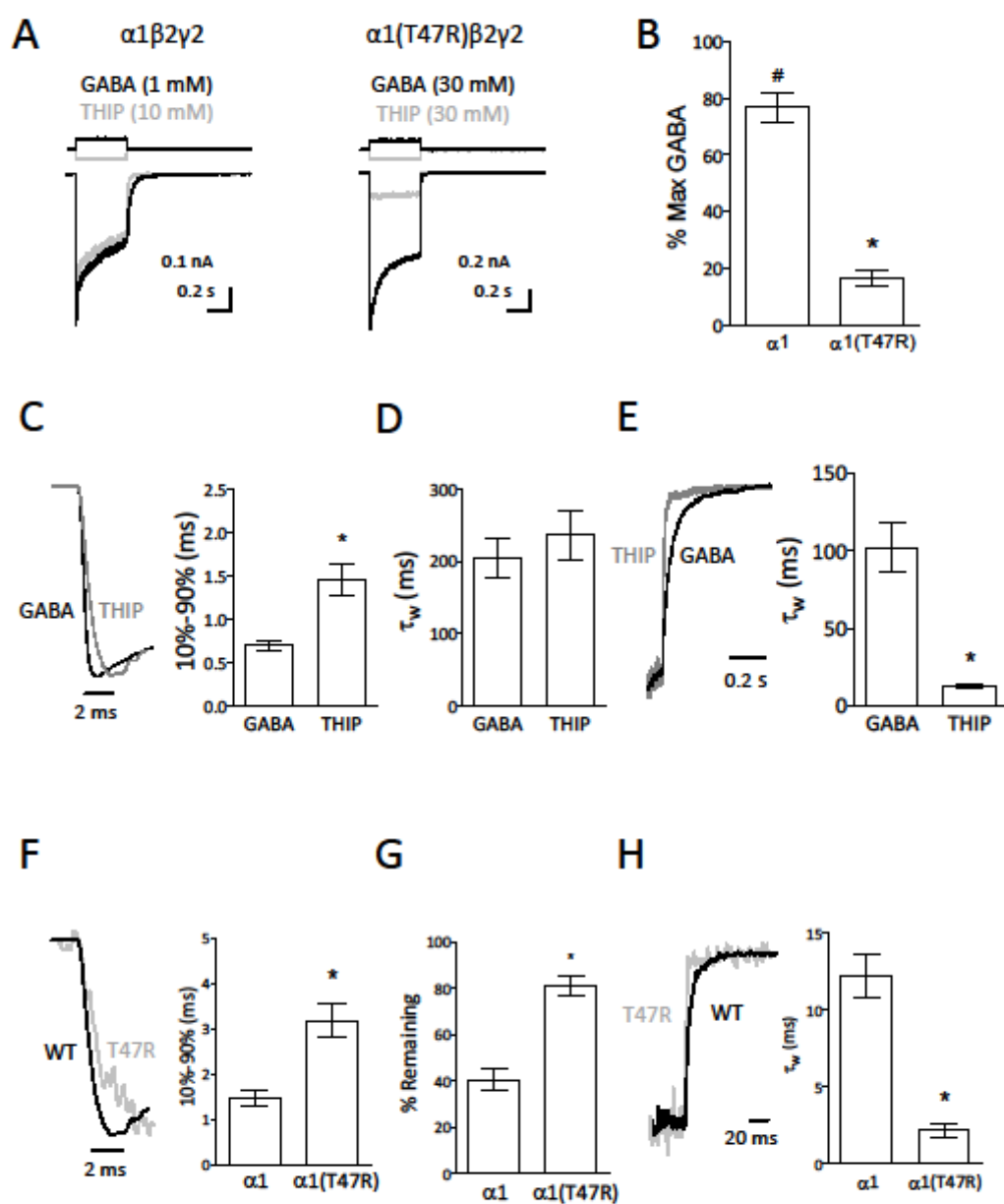


Fig. 6

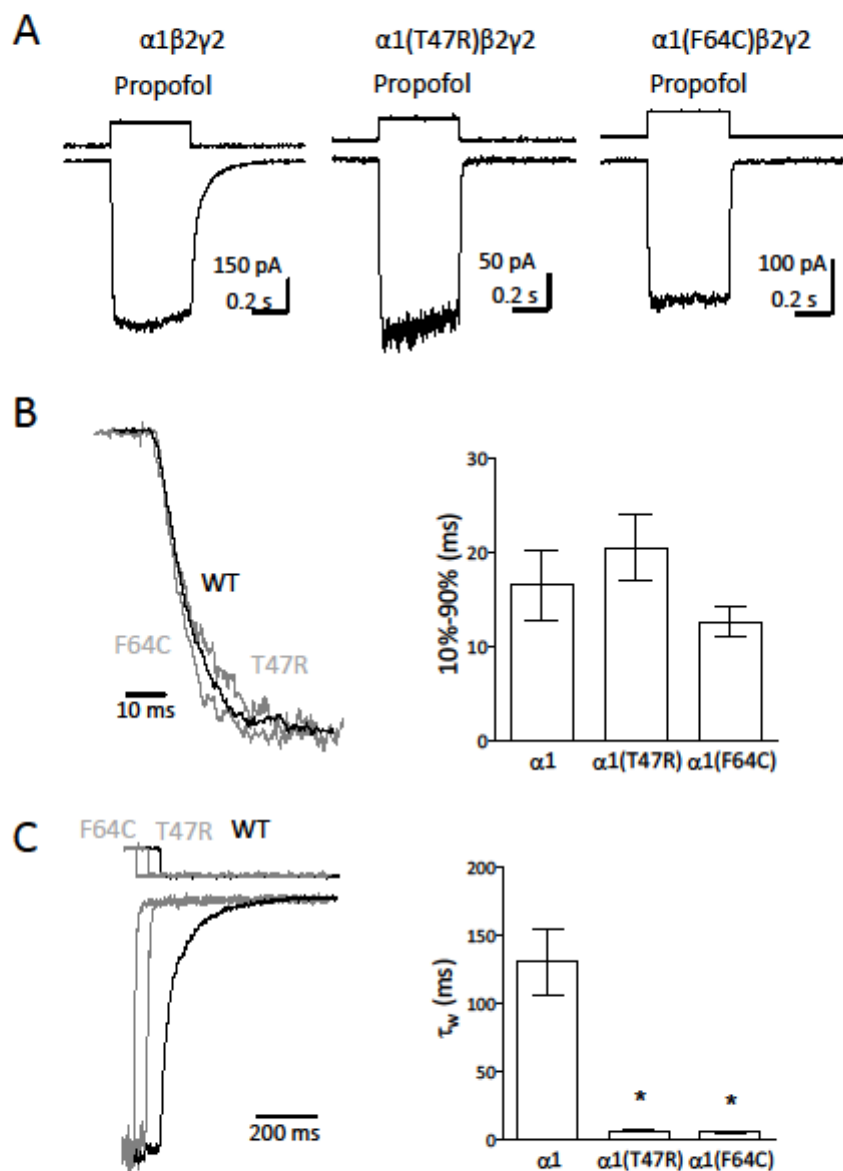


Fig. 7

